

Aus dem Institut für Klinische Radiologie der Ludwig-Maximilians-Universität München

Direktor: Prof. Dr. med. Dr. h.c. M. Reiser, FACR, FRCR

**Morphologische und funktionelle Bildgebung mittels hochauflösender
3.0 Tesla Multi-Sequenz Magnetresonanztomographie und
18F-Fluorodesoxyglukose PET Computertomographie bei Patienten mit
spontanen Dissektionen der Halsgefäße**

Dissertation
zum Erwerb des Doktorgrades der Medizin
an der Medizinischen Fakultät der
Ludwig-Maximilians-Universität zu München

vorgelegt von
Maximilian Habs
aus Heidelberg
2012

Mit Genehmigung der Medizinischen Fakultät
Der Universität München

Berichterstatter: Prof. Dr. med. Konstantin Nikolaou

Mitberichterstatter: Prof. Dr. med. Gerhard F. Hamann
Prof. Dr. med. Thomas N. Witt

Mitbetreuung durch den
promovierten Mitarbeiter: PD Dr. med. Tobias Saam

Dekan: Prof. Dr. med. Dr. h.c. Maximilian F. Reiser, FACR, FRCR

Tag der mündlichen Prüfung: 29.11.2012

Meinen Eltern in Dankbarkeit

Inhaltsverzeichnis

1. EINLEITUNG	5
1.1. Spontane Dissektionen der Halsgefäße	5
1.2. Hochauflösende Multi-Sequenz MRT in der Bildgebung der Halsgefäße	8
1.3. 18F-Fluorodesoxyglukose PET Computertomographie in der Diagnostik von entzündlichen Gefäßerkrankungen	9
1.4. Zielsetzung der Arbeiten	10
1.5. Zusammenfassung der vorliegenden Arbeiten	12
1.6. Summary of the presented publications	15
1.7. Literaturangaben	17
2. ERGEBNISSE	21
2.1. Publikation Pfefferkorn T., Habs M. et al., Stroke 2011	22
2.2. Publikation Habs M. et al., JCMR 2011	44
3. VERÖFFENTLICHUNGEN	67
4. DANKSAGUNGEN	70
5. LEBENSLAUF	71

1. EINLEITUNG

1.1. Spontane Dissektionen der Halsgefäße

Als Dissektion (lat. *dissecare*: „zerschneiden“) einer Schlagader wird in der Medizin die Spaltung der Gefäßwand durch ein Wandhämatom bezeichnet. Dissektionen können in allen großen Arterien, sowie der Aorta auftreten. Bei der Dissektion der Halsarterien (*A. carotis* und *A. vertebralis*) führt in der Regel ein Riss der inneren Gefäßwand zum Eintritt von Blut zwischen die Schichten der Gefäßwand¹. Des Weiteren wird eine Blutung der *vasa vasorum* der jeweiligen Arterie als mögliche Ursache für Dissektionen der Halsgefäße angenommen. Je nachdem zwischen welchen Schichten sich das Wandhämatom ausbildet, führt dies entweder zu einer Stenose (Dissektion zwischen *tunica intima* und *tunica media*) oder zu einer aneurysmatischen Erweiterung des Gefäßes (Dissektion zwischen *tunica media* und *tunica adventitia*)². Die Komplikationen einer Dissektion sind Gefäßokklusion, Thrombembolie oder extravasale Blutung³. Als Folge kann hieraus eine transitorische ischämische Attacke (TIA) oder ein ischämischer Schlaganfall entstehen. Insbesondere bei Jugendlichen und Personen im mittleren Lebensalter ist die Dissektion der Halsgefäße eine häufige Ursache für ischämische Schlaganfälle⁴. Das mittlere Erkrankungsalter liegt für Männer und Frauen bei ca. 45 Jahren, eine Geschlechterpräferenz gibt es nicht⁵.

Es werden spontane von traumatischen Dissektionen unterschieden. Bei den traumatischen Dissektionen existiert ein adäquates Trauma in der Vorgeschichte (z.B. Verkehrsunfall)¹. Die Ätiologie der spontanen Dissektion der Halsgefäße ist bisher unbekannt und wahrscheinlich multifaktoriell⁶. Es konnten prädisponierende Faktoren für eine spontane Dissektion der Halsgefäße identifiziert werden, diese sind teils genetisch und teils umweltbezogen. Patienten mit bestimmten Bindegewebserkrankungen (z.B. Ehlers-Danlos-Syndrom) erleiden häufiger eine Dissektion als die Normalbevölkerung⁷. Zudem zeigten Patienten mit Dissektion häufiger Infektionen der Atemwege in der medizinischen Vorgeschichte⁸. Traditionelle kardiovaskuläre Risikofaktoren (z.B. Hypertonie, Rauchen, Diabetes, Hyperlipidämie) sind nicht mit der Erkrankung assoziiert⁹. Die Inzidenz von spontanen Karotidisdissektionen und Vertebralisdissektionen liegt zusammen bei ca. 5 pro 100 000 Personen und ist im Herbst und Winter höher¹⁰. Der genaue Grund für den Gipfel der Inzidenz in der kalten

Jahreszeit ist unklar, jedoch wird auch hier eine Assoziation mit gehäuften Infektionen zu dieser Jahreszeit angenommen¹¹.

Die Symptomatik eines Patienten mit Dissektion hängt von dem betroffenen Gefäß ab. Dennoch gibt es eine Trias von Symptomen, welche bei Patienten mit Dissektion sehr oft vorkommen: Kopf- und Nackenschmerzen, Horner-Syndrom (Ptosis, Miosis, Enophthalmus) und cerebrale Ischämie. In Studien wurden bei ca. 70 % der Patienten mit Dissektion eine cerebrale Ischämie (TIA oder Schlaganfall) festgestellt^{2, 12}. Wenn der klinische Verdacht auf eine Dissektion besteht, dann ist die bildgebende Diagnostik entscheidend, um das Dissektionssegment, das Wandhämatom und die Lumenirregularität des Gefäßes darzustellen. Hierbei kommen Ultraschall, Magnetresonanztomographie (MRT), Computertomographie (CT) und digitale Subtraktionsangiographie (DSA) zum Einsatz. Die Bedeutung der invasiven DSA in der Diagnostik von Dissektionen hat in den letzten Jahren stark abgenommen. Dies beruht einerseits auf der guten Sensitivität und Spezifität für das Erkennen der Dissektionen von neueren nicht-invasiven Verfahren (z.B. MRT oder CT), als auch auf der Tatsache, dass das Wandhämatom mit der DSA nicht direkt dargestellt werden kann. Die farbkodierte Dopplersonographie (FKDS) ist bei extrakraniellen Karotidisdissektionen eine schnelle und kostengünstige Methode, welche besonders Veränderungen des Blutflusses und Gefäßstenosen mit hoher diagnostischer Sicherheit erfasst. Sie ist ein geeignetes Verfahren für die initiale Diagnostik und ermöglicht auch die Visualisierung der Gefäßwand¹³. Nachteile der FKDS sind neben der Untersucherabhängigkeit vor allem die schlechte Abbildung der *Aa. vertebrales* in den *foramina transversaria* der Halswirbel sowie der intrakraniellen Abschnitte der *A. carotis interna*⁴. Die diagnostische Modalität der Wahl bei Dissektion der Halsgefäße sollte nach aktueller Leitlinie die MRT (bei 1,5 oder 3,0 Tesla) mit Kontrastmittel-Angiographie (MRA) sein¹⁴. Diese Untersuchung ist nicht invasiv und mit keiner Strahlenbelastung verbunden. Charakteristisch für eine Dissektion im MR-tomographischen Schnittbild ist hier ein halbmondförmiges, in fettsupprimierten T1-gewichteten Sequenzen *hyperintenses* Wandhämatom, welches meist das Lumen exzentrisch einengt. An dieser Stelle sei erwähnt, dass sich die Signalintensitäten von Hämatomen in der MRT mit der Zeit verändern¹⁵. Dies beruht auf den MR-Signaleigenschaften des Hämoglobins und dessen schrittweisen Abbaus im Hämatom. Erst in der subakuten Phase (nach ca. 1-3 Tagen) wird das Wandhämatom in der MRT gut sichtbar³. Die Sensitivität und Spezifität der MRT/MRA ist sehr gut für das Erkennen von Karotidisdissektionen, jedoch nur mäßig bei Vertebralisdissektionen¹⁶.

Ein weiterer Vorteil der MRT besteht darin, dass während der Messung auch das Gehirn mituntersucht werden kann. Diffusionsgewichtete Sequenzen können zeigen, ob gleichzeitig eine cerebrale Ischämie vorliegt. Bestehen Kontraindikationen zur MRT (z.B. Herzschrittmacher), oder war die MRT nicht konklusiv, dann kann eine CT-Angiographie (CTA) der Halsgefäße erwogen werden. Die diagnostische Sicherheit der CTA ist jedoch niedriger als bei der MRT/MRA, da mit dieser Methode nur die Stenose bzw. Gefäßirregularität und ggfs. ein Dissektionssegel erkannt werden können. Das Wandhämatom selbst ist mit der CT jedoch nur eingeschränkt darstellbar. Ein weiterer Nachteil der CTA ist die mit dieser Methode assoziierte Strahlenbelastung, bei in der Regel relativ jungen betroffenen Patienten.

Konnte bei einem symptomatischen Patienten eine Dissektion in der Bildgebung nachgewiesen werden, dann erfolgt eine präventive Behandlung zur Vermeidung von vaskulären Komplikationen. Im Zentrum der Akutversorgung einer Dissektion der Halsgefäße steht die anti-thrombembolische Therapie. Ob dies besser durch Thrombozytenaggregationshemmer (z.B. Acetylsalicylsäure) oder durch Inhibitoren der plasmatischen Gerinnung (z.B. Heparin) erfolgen sollte, ist derzeit noch nicht sicher geklärt¹⁷. Große Meta-Analysen von Studien konnten keinen signifikanten Unterschied zwischen Thrombozytenaggregationshemmern und Antikoagulantien in Bezug auf Mortalität, Komplikationen und Langzeitergebnisse zeigen¹⁸. In Deutschland werden die Patienten üblicherweise zunächst mit Heparin therapiert (PTT: 2-3-fach verlängert), und dann für 3 bis 6 Monate mit Vitamin K Antagonisten weiterbehandelt (Ziel-INR: 2,0-3,0). Zeigen konventionelle Therapiestrategien keinen Erfolg, kann eine endovaskuläre Intervention mit Stentimplantation indiziert sein¹⁹.

Insgesamt haben Dissektionen der Halsgefäße eine gute Langzeitprognose² und heilen über einen Zeitraum von 3-6 Monaten meist von selbst aus³. Nach dem Erstereignis der Dissektion wird im weiteren Verlauf zwischen einem Rezidiv der Dissektion und einem Rezidiv der cerebralen Ischämie unterschieden. Ein erneutes Auftreten einer Dissektion, auch an einer anderen Halsarterie, ist insbesondere in den ersten Monaten nach der initialen Dissektion möglich und wird in der Literatur mit bis zu 19% im ersten Monat angegeben^{20, 21}. Diese sekundären Dissektionen sind meist asymptomatisch und werden oft zufällig in einer MRT-Verlaufskontrolle festgestellt. Das Risiko für einen erneuten Schlaganfall nach Dissektion ist gering²². Die Veränderungen der Gefäßwand (z.B. Stenose, Wandhämatom) bilden sich im Verlauf fast vollständig zurück und die meisten Patienten zeigen keine bleibenden neurologischen Defizite².

1.2. Hochauflösende Multi-Sequenz MRT in der Bildgebung der Halsgefäße

Mit immer höheren Feldstärken und immer sensitiveren Spulenelementen wurde die räumliche Auflösung und Gewebekontrastierung der MRT in den letzten Jahren stetig besser. Die MRT ist für die Darstellung der Halsgefäße sehr gut geeignet, da die Strukturen oberflächlich liegen und sich kaum bewegen. Durch dedizierte Oberflächenspulen, welche direkt am Hals angebracht werden, kann das Signal-Rausch-Verhältnis (SNR) deutlich verbessert werden und man erhält hochauflösende Bilder der Gefäßwand in vivo. Hochauflösend bedeutet in diesem Kontext eine Pixelgröße von $< 500 \times 500$ Mikrometer²³. Zudem ermöglicht die kontrastmittelverstärkte MR-Angiographie (CE-MRA) eine Beurteilung des Gefäßlumens. Bei der CE-MRA wird gadoliniumhaltiges Kontrastmittel intravenös appliziert. Aufgrund der paramagnetischen Eigenschaften von Gadolinium entsteht durch T1-Zeit-Reduktion ein deutliches Signal im Gefäß auf T1-gewichteten 3D Sequenzen. Liegt eine relevante Engstelle ($> 70\%$ Durchmesserstenose) im Gefäß vor, wird sie mittels CE-MRA mit hoher diagnostischer Sicherheit erkannt²⁴. Neben kontrastmittelverstärkten Verfahren gibt es auch MR-Angiographien, welche keine Kontrastmittelgabe erfordern²⁵. Diese so genannten „bright blood“ Sequenzen (z.B. time-of-flight MRA) sind deshalb besonders für Patienten mit eingeschränkter Nierenfunktion geeignet. Trotz guter Bildqualität ist die time-of-flight MRA der CE-MRA in der Diagnostik von Gefäßengstellen etwas unterlegen und der Schweregrad der Stenose wird häufig überschätzt. Dem gegenüber stehen „black blood“ Sequenzen, bei welchen das MR-Signal des Blutes im Gefäß unterdrückt wird und ein guter Kontrast zwischen dem nun *hypointensem* Lumen und der Gefäßwand entsteht. Bei der „black-blood“ Technik werden meist fettsupprimierte turbo-spin-echo (TSE) Sequenzen eingesetzt, die zur Flussunterdrückung einen vorzeitigen Sättigungsimpuls (double inversion recovery = DIR) entlang der Richtung des arteriellen Blutflusses einsetzen²⁶. Diese Sequenzen können T1, T2 oder nach Protonendichte (PD) gewichtet sein. Die wechselnden Signaleigenschaften von Gewebe in den unterschiedlich gewichteten Sequenzen erlaubt die Differenzierung von verschiedenen Gewebetypen (z.B. Fett, Bindegewebe, Verkalkungen)²³.

Extrazelluläre MR-Kontrastmittel (z.B. Gadobutrol) ermöglichen den Vergleich von nativen T1-gewichteten Sequenzen und T1-gewichteten Sequenzen mehrere Minuten nach Kontrastmittelapplikation. Mit der Zeit verlässt das gadoliniumhaltige Kontrastmittel den Intravasalraum und hyperperfundierte Gewebe oder Gewebe mit erhöhter Gefäßpermeabilität

kommen nun *hyperintens* zur Darstellung. Damit können insbesondere entzündliche Prozesse in der Gefäßwand visualisiert werden²⁶.

Die hochauflösende Multi-Sequenz MRT wird seit Ende der 90er Jahren zunehmend in der Charakterisierung von atherosklerotischen Plaques in den Karotiden eingesetzt. Mit ihrer Hilfe können Plaquekomponenten in vivo identifiziert werden, was eine Abschätzung des Risikos für einen Schlaganfall erlaubt („vulnerable Plaque“)²⁷. Vor allem die Einblutung eines Karotisplaques gilt als Zeichen für Vulnerabilität und kann in der MRT mit guter Sensitivität und Spezifität im Vergleich zur Histopathologie erkannt und nach Alter klassifiziert werden²⁸. Neben diesem sogenannten *Plaqueimaging* bei Atherosklerose der Halsarterien wurden in den letzten Jahren zunehmend auch andere cervikale Arteriopathien mittels der Multi-Sequenz MRT untersucht. So zeigte sich, dass bei Vaskulitiden (z.B. Riesenzellarteriitis) mit entzündlichen Veränderungen der Gefäßwand kontrastmittelverstärkte MRT Sequenzen eine Aussage über das Ausmaß und die Aktivität der Erkrankung ermöglichen²⁹. Auch in der Diagnostik von Dissektionen der Halsarterien hat die MRT/MRA große Fortschritte gemacht und die konventionelle digitale Subtraktionsangiographie fast völlig ersetzt. Bei Dissektionen kann die MRT die Ausdehnung und das Alter des Wandhämatoms abschätzen.

Aktuell liegt die Akquisitionszeit bei paralleler Bildgebung für eine hochauflösende Multi-Sequenz MRT der Halsgefäße bei ca. 15-20 min pro Patient^{26, 30}. Für den Nachweis einer Dissektion kann auf die Gabe von gadoliniumhaltigem Kontrastmittel verzichtet werden, da zur Darstellung des Wandhämatoms alleinige fett-supprimierte T1-gewichtete Sequenzen ausreichen.

1.3. 18F-Fluorodesoxyglukose PET Computertomographie in der Diagnostik von entzündlichen Gefäßerkrankungen

Die Positronen-Emissions-Tomographie (PET) CT bedient sich eines radioaktiv markierten Tracers (18-F-FDG) und kombiniert morphologische und funktionelle Bildgebung. Entzündete Gewebe nehmen aufgrund der erhöhten Leukozytenaktivität vermehrt Glukose aus dem Blut auf. 18F-FDG wird wie normale Glukose über Transporter in die Zellen aufgenommen und phosphoryliert. Da die radioaktiv markierte Glukose nicht in der Glykolyse verwertet wird, reichert sie sich in Geweben mit hoher Stoffwechselaktivität an und kann detektiert werden³¹. Mit Hilfe einer Computersoftware wird die Aktivität quantifiziert und meist als SUV (standardized uptake value) innerhalb einer Region (ROI = region of interest) wiedergegeben. Der SUV

berechnet sich aus der Aktivitätskonzentration (in kBq/ml) geteilt durch die applizierte Aktivität pro Kilogramm Körpergewicht (in kBq/kg). Häufig wird auch der TBR-Wert angegeben (TBR = target to background ratio), welcher das Verhältnis von maximalem SUV in der ROI zu dem mittleren SUV im venösen Blut beschreibt (z.B. gemessen in der *V. cava inferior*). Da die räumliche Auflösung der erhaltenen PET-Datensätze begrenzt ist, ermöglicht erst die Korrelation mit der CT die Zuordnung zu anatomischen Strukturen.

Im Bereich des Gefäßsystems wird die FDG-PET/PET-CT vor allem in der Diagnostik von Großgefäßvaskulitiden und Atherosklerose eingesetzt. FDG-PET/PET-CT Studien bei Patienten mit Großgefäßvaskulitis konnten nicht nur die befallenen Arterien identifizieren, sondern auch die Krankheitsaktivität vor und während der Therapie beurteilen³²⁻³⁴. Da auch Atherosklerose eine vaskuläre Entzündung repräsentiert, kann mittels PET-CT der Metabolismus in atherosklerotischen Plaques der großen Gefäße dargestellt werden (z.B. Aorta, Karotiden, Iliakalgefäße). Die erhöhte entzündliche Aktivität gilt hierbei selbst als Risikofaktor für eine Plaqueruptur und kardiovaskuläre Komplikationen³⁵. Der 18F-FDG Uptake im Gefäßsystem korreliert sowohl mit der Anzahl an individuellen kardiovaskulären Risikofaktoren^{36, 37}, als auch mit einigen vulnerablen Eigenschaften (z.B. Einblutung) der atherosklerotischen Plaques selbst^{38, 39}. Der größte Nachteil der PET-CT Diagnostik ist neben den relativ hohen Kosten die Strahlenbelastung der Patienten. Diese reicht von 6-7 mSv pro FDG-PET und 14-18 mSv pro CT Untersuchung. Häufig kann die Strahlenbelastung der CT durch ein low-dose Protokoll (2-5 mSv) reduziert werden⁴⁰.

1.4. Zielsetzung der Arbeiten

Ziel unserer Studien war es, durch die hochauflösende MRT und die 18F-Fluorodesoxyglukose PET-CT, neben der bildmorphologischen Diagnose der Dissektion, auch neue pathophysiologische Erkenntnisse über die Erkrankung zu gewinnen. Die Idee hierfür kam durch eine Beobachtung bei einer 42-jährigen Patientin mit multiplen spontanen Dissektionen der Halsarterien, die in der Multi-Sequenz MRT eine ausgeprägte entzündliche Reaktion im Bereich der Gefäße zeigten. Bei Verdacht auf Vaskulitis wurde bei der Patientin eine PET-CT Untersuchung durchgeführt, welche eine generalisierte Gefäßentzündung bestätigte, jedoch keine, für eine Großgefäßvaskulitis typischen Veränderungen nachweisen konnte. Da bereits bekannt war, dass spontane Dissektionen der Halsarterien mit systemischen Entzündungszeichen (z.B.

erhöhtes C-reaktives Protein im Serum) assoziiert sind⁴¹, und auch histologische Studien eine generalisierte Veränderung der Gefäßarchitektur zeigten⁴², wollten wir gezielt in diesem Patientenkollektiv die Entzündungsaktivität im Bereich des Aortenbogens und der supraaortalen Arterien erfassen. Die hochauflösende Multi-Sequenz MRT ist für diese Fragestellung besonders geeignet, da sie nicht-invasiv entzündliche Gefäßwandveränderungen darstellen kann (z.B. Gefäßwandverdickung und perivaskuläres Ödem), sowie Hinweise für erhöhte Gewebepfusion in KM-Sequenzen finden kann. Insbesondere sollte die Ausdehnung (lokal vs. generalisiert) der entzündlichen Gefäßwandveränderungen analysiert werden. Zur Korrelation der MRT Befunde mit der tatsächlichen Entzündungsaktivität im Bereich der Gefäßwände diente die PET-CT, welche ebenfalls jeder Patient mit frischer Dissektion erhalten sollte. Von Interesse waren hier auch Subgruppen von Patienten (z.B. Patienten mit multiplen Dissektionen), die womöglich eine stärker ausgeprägte Form der Erkrankung zeigen. Für jeden Patienten wurde eine MRT und/oder PET-CT Verlaufskontrolle nach wenigen Monaten geplant. Die Hypothese, dass sich bei Patienten mit spontaner Dissektion eine transiente generalisierte Gefäßentzündung findet, ist vor allem deshalb relevant, da antiinflammatorische Therapiestrategien hier den Verlauf beeinflussen könnten.

Ein weiteres Ziel war es, die mittels MRT erhaltenen Daten morphologisch exakt zu beschreiben und bei der Bildanalyse die Wandhämatome durch deren MR-Signalcharakteristika nach ihrem Alter einzustufen. Lokalisation, Stenosegrad und MR-morphologisches Alter des Wandhämatoms sollten mit klinischen Parametern (z.B. Symptomatik) korreliert werden. Das Verhalten von Hämatomen und ihrem sequentiellen Abbau in der MRT über die Zeit ist bei intrakraniellen Blutungen gut erforscht. Während des Abbaus von Hämoglobin und Erythrozyten verändert das Hämatom seine Signalintensität in T1- und T2-gewichteten Sequenzen. Auch bei MRT *Plaqueimaging* Studien von atherosklerotisch veränderten Gefäßen konnten unterschiedliche Einblutungstypen nach Alter unterschieden werden²⁸. Histologisch werden Einblutungen von Karotisplaques in frische, subakute und alte Einblutungen klassifiziert, wobei frische Einblutungen 1-7 Tage, subakute Einblutungen 8-42 Tage und chronische Einblutungen >42 Tage alt sind⁴³. Da zwar die Veränderungen der MR-Signalcharakteristika in T1- und T2-gewichteten Sequenzen über die Zeit auch für Wandhämatome von Dissektionen bekannt sind⁴⁴, jedoch noch nie zuvor eine systematische Untersuchung an einem größeren Patientenkollektiv durchgeführt wurde, haben wir versucht ein durchschnittliches Alter für bestimmte MR-Entitäten

von Wandhämatome zu beschreiben. Dies ist auch von klinischem Interesse, da eine Unterscheidung zwischen frischer und alter Dissektion ermöglicht wird und ein Zeitfenster für die Entstehung der Dissektion angegeben werden kann.

1.5. Zusammenfassung der vorliegenden Arbeiten

Zwischen 2007 und 2010 wurden mehr als 50 Patienten mit Dissektionen der Halsgefäße mittels neuem, für Dissektionen modifiziertem Multi-Sequenz MRT-Protokoll und 18F-Fluorodesoxyglukose PET-CT an unserem Institut für Klinische Radiologie in Großhadern untersucht. In dieser prospektiven mono-zentrischen Beobachtungsstudie wurden alle Messungen an einem 3.0 Tesla Scanner (Magnetom Verio; Siemens Healthcare) und an zwei PET-CT Scanner (Philips Gemini; Philips Healthcare und Siemens Biograph 64; Siemens Healthcare) durchgeführt. Die Studie erfolgte in enger Kooperation mit der Neurologischen Klinik und Nuklearmedizinischen Klinik. Es wurden für jeden Patienten detaillierte anamnestische und klinische Daten erhoben.

Das MRT Protokoll umfasste für jeden Patienten eine time-of-flight Angiographie, fettgesättigte T1- und T2-gewichtete *black-blood* Sequenzen vor und T1-gewichtete Sequenzen nach Kontrastmittelapplikation (Gadovist®, Bayer-Schering). Mit einer maximalen Auflösung $0,5 \times 0,5 \text{ mm}^2$ wurden die supraaortalen Gefäße vom Aortenbogen bis zu der Schädelbasis abgebildet. Jeder Patient wurde durch diffusionsgewichtete Sequenzen des Schädels auf das Vorhandensein von cerebralen Ischämien untersucht. Die selben Patienten erhielten ebenfalls eine 18F-Fluorodesoxyglukose PET-CT der thorakalen und zervikalen Gefäße. Um die Strahlenbelastung der Patienten gering zu halten, wurde eine low-dose CT durchgeführt. Die Messung der SUVs im Gefäßsystem erfolgte eine Stunde nach Applikation des Tracers (Aktivität: 5 MBq/kg KG). Die berechnete effektive Dosis betrug 8 mSv pro Patient. Neben der quantitativen PET-CT Auswertung erfolgte sowohl für die PET-CT als auch für die MRT Untersuchung eine qualitative Analyse durch erfahrene Radiologen mit der Frage nach dem Ausmaß entzündlicher Gefäßveränderungen. Hierbei wurden lokale von generalisierten Gefäßentzündungen unterschieden.

Für die Studie von *Pfefferkorn T. et al in Stroke 2011* konnten letztendlich 37 konsekutive Patienten mit spontanen Dissektionen der Halsarterien eingeschlossen werden. PET-CT-Untersuchungen von 27 Patienten (82%) wiesen eine signifikante perivaskuläre FDG-Aufnahme

im Bereich der arteriellen Dissektion auf, die bei 8 Patienten (24%) nicht auf den Bereich der arteriellen Dissektion beschränkt war. Wir fanden eine starke positive Korrelation zwischen dem Vorhandensein einer Dissektion und perivaskulärer Kontrastmittelaufnahme (Pearson's $R=0,73$; $p<0,001$) und perivaskulärem Ödem ($R=0,65$; $p<0,001$) in der MRT. Alle Patienten mit entzündlichen Veränderungen im MRT und/oder PET-CT wiesen nach 3 Monaten eine spontane Remission der perivaskulären entzündlichen Veränderungen auf. Diese Studie zeigt, dass bei Patienten mit spontane Dissektionen der Halsarterien im Bereich der Dissektion häufig entzündliche Veränderungen nachgewiesen werden können. In einem kleineren Teil der Patienten sind diese entzündlichen Veränderungen nicht nur im Bereich der Dissektion sondern auch in anderen arteriellen Gefäßen zu finden, was eine entzündliche Pathogenese bei einem Teil der Patienten suggeriert.

In die Studie über die Altersbestimmung von Wandhämatomen bei spontanen Dissektionen der Halsarterien von *Habs M. et al in JCMR 2011* konnten 35 Patienten eingeschlossen werden. Die Wandhämatome wurden basierend auf deren relativen Signalintensitäten in den T1- und T2-gewichteten Sequenzen klassifiziert und als akut, früh subakut, spät subakut und chronisch beschrieben. Es wurden nur Patienten in die Studie aufgenommen bei denen das Alter der Dissektion anhand der klinischen Symptome (Horner-Syndrom, TIA oder Schlaganfall) bestimmt werden konnte. Basierend auf der MRT-Klassifikation unterschied sich das mittlere Alter früher subakuter Einblutungen, später subakuter Einblutungen und chronischer Einblutungen signifikant voneinander (5,8 vs. 15,7 vs. 58,7 Tage). Es zeigte sich eine sehr gute Übereinstimmung zwischen der MRT-basierten Klassifikation und dem Alter der Einblutungen (Cohen's kappa 0,74; $p<0,001$). Die Signalintensitäten der Wandhämatome bei Dissektion unterscheiden sich je nach Alter der Einblutung. Diese Information kann hilfreich sein, wenn das genaue Alter der Dissektion bei unspezifischer klinischer Symptomatik nicht bekannt ist.

Beitrag des Doktoranden zu den publizierten Arbeiten:

Die Idee und das Konzept der Studien wurden von Dr. Tobias Saam und Dr. Thomas Pfefferkorn entwickelt. Der Doktorand Maximilian Habs war für die Patientenakquisition und die MRT Messungen zuständig. Des Weiteren war er in die statistische Datenauswertung und Manuskriptverfassung involviert. Die nuklearmedizinischen Messungen wurden durch Dr. Marcus Hacker und Dr. Axel Rominger geleitet. Prof. Dr. Konstantin Nikolaou und Prof. Dr. Dr. h.c. Maximilian Reiser betreuten und unterstützten das gesamte Projekt.

1.6. Summary of the presented publications

Between 2007 and 2010 more than 50 patients with spontaneous dissections of cervical arteries have been examined and scanned with a modified cervical MRI and fluorodeoxyglucose (^{18}F) PET CT protocol at the Institute of Clinical Radiology, LMU Munich. Within this prospective, mono-centric study all imaging data was obtained by using a 3.0 tesla scanner (Magnetom Verio; Siemens Healthcare) and two PET CT scanners (Philips Gemini; Philips Healthcare and Siemens Biograph 64; Siemens Healthcare). This study was based on and conducted by a strong cooperation between the Department of Neurology and the Department of Nuclear Medicine. Detailed data sets regarding patient history and clinical parameters were recorded for every patient.

The MRI protocol included a time-of-flight angiography, fat-saturated T1- and T2-weighted *black-blood* sequences before and after the administration of contrast medium (Gadovist®, Bayer-Schering). The scans covered the supra-aortic vessels from the aortic arch to the base of the skull with a best in plane resolution of $0.5 \times 0.5 \text{ mm}^2$. Every patient received an additional diffusion-weighted brain-MRI for evaluation of ischemia. The supra-aortic vessels of the same patients were also scanned by a low dose FDG/PET-CT. Measurements of standardized uptake values for every vessel segment were obtained after the administration of the tracer (activity: 5 MBq/kg bodyweight). The calculated effective dose was 8 mSv per patient. Along with quantitative PET-CT analysis, experienced radiologists performed qualitative evaluation of vessel wall inflammation for PET-CT and the MR images. Local inflammatory changes at the site of dissection were distinguished from generalized inflammation of the vascular system.

For the study of *Pfefferkorn et al (Stroke 2011)* 37 patients with spontaneous cervical dissection matched the inclusion criteria. In 27 patients (83%) PET-CT showed significant perivascular FDG-uptake at the site of dissection. 8 Patients (24%) showed signs of generalized inflammation with increased FDG-uptake at additional vessel segments (e.g. aortic arch). We found a strong positive correlation between the presence of dissection and perivascular contrast enhancement (Pearson's $r=0.73$; $p<0.001$) and perivascular edema ($r=0.65$; $p<0.001$) as determined by MRI. All Patients with inflammatory changes seen by MRI and/or PET-CT showed complete remission in the follow-up scan after 3 month. This study demonstrated the high prevalence of inflammatory changes at the site of dissection, which can be detected by MRI

and PET-CT. Furthermore the study showed that generalized vessel wall inflammation is present in small subgroup of patients, suggesting that vascular inflammation plays an important role in the pathogenesis of cervical artery dissections.

The study of *Habs et al (JCMR 2011)* investigated the age determination of vessel wall hematomas by MRI in 35 patients with spontaneous cervical artery dissection. The vessel wall hematomas were classified according to their relative signal intensities on T1- and T2-weighted images and were described as either acute, early subacute, late subacute or chronic. Only patients with a clear clinical onset of symptoms typical for cervical artery dissection (e.g. Horner's syndrome, TIA, stroke) were included in this study, so that the age of the dissection could be determined. Based on the MRI assessment of the vessel wall hematomas the mean age of the dissection for early subacute, late subacute and chronic appearance of the hematoma differed significantly from each other (5.8 vs. 15.7 vs. 58.7 days). There was a strong agreement between the MRI based classification and the age of the hematoma (Cohen's kappa 0.74; $p < 0.001$). In a nutshell, MR signal intensities of vessel wall hematomas in patients with cervical artery dissections change over time, which can be a useful tool to evaluate the age of a dissection in patients with unclear onset of symptoms or unspecific presentation.

Doctorate candidate's contributions to the publications:

The idea for this project and the study design came from Dr. Tobias Saam and Dr. Thomas Pfefferkorn. The doctorate candidate Maximilian Habs was involved in the patient care and acquisition, performing MRI scans, statistical analysis and writing the manuscript. Dr. Marcus Hacker and Dr. Axel Rominger conducted and analyzed the PET-CT scans. Prof. Dr. Konstantin Nikolaou and Prof. Dr. Dr. h.c. Maximilian Reiser supervised and supported the whole project.

1.7. Literaturangaben

1. Schievink WI. Spontaneous dissection of the carotid and vertebral arteries. *N Engl J Med*. 2001;344:898-906
2. Kim YK, Schulman S. Cervical artery dissection: Pathology, epidemiology and management. *Thromb Res*. 2009;123:810-821
3. Fusco MR, Harrigan MR. Cerebrovascular dissections--a review part i: Spontaneous dissections. *Neurosurgery*. 2011;68:242-257; discussion 257
4. Debette S, Leys D. Cervical-artery dissections: Predisposing factors, diagnosis, and outcome. *Lancet Neurol*. 2009;8:668-678
5. Arnold M, Kappeler L, Georgiadis D, Berthet K, Keserue B, Boussier MG, Baumgartner RW. Gender differences in spontaneous cervical artery dissection. *Neurology*. 2006;67:1050-1052
6. Schievink WI, Debette S. Etiology of cervical artery dissections: The writing is in the wall. *Neurology*. 2011;76:1452-1453
7. Grond-Ginsbach C, Debette S. The association of connective tissue disorders with cervical artery dissections. *Curr Mol Med*. 2009;9:210-214
8. Grau AJ, Brandt T, Forsting M, Winter R, Hacke W. Infection-associated cervical artery dissection. Three cases. *Stroke*. 1997;28:453-455
9. Rubinstein SM, Peerdeman SM, van Tulder MW, Riphagen I, Haldeman S. A systematic review of the risk factors for cervical artery dissection. *Stroke*. 2005;36:1575-1580
10. Paciaroni M, Georgiadis D, Arnold M, Gandjour J, Keseru B, Fahrni G, Caso V, Baumgartner RW. Seasonal variability in spontaneous cervical artery dissection. *J Neurol Neurosurg Psychiatry*. 2006;77:677-679
11. Schievink WI, Roiter V. Epidemiology of cervical artery dissection. *Front Neurol Neurosci*. 2005;20:12-15
12. Lee VH, Brown RD, Jr., Mandrekar JN, Mokri B. Incidence and outcome of cervical artery dissection: A population-based study. *Neurology*. 2006;67:1809-1812
13. Benninger DH, Georgiadis D, Gandjour J, Baumgartner RW. Accuracy of color duplex ultrasound diagnosis of spontaneous carotid dissection causing ischemia. *Stroke*. 2006;37:377-381
14. H. C. Diener NP, P. Berlit, G. Deuschl, E. Elger, R. Gold, W. Hacke, A. Hufschmidt, H. Mattle, U. Meier, W. H. Oertel, H. Reichmann, E. Schmutzhard, E. W. Wallesch, M. Weller. Leitlinien für diagnostik und therapie in der neurologie; 4. Überarbeitete auflage. *AWMF online*. 2011

15. Grossman RI, Gomori JM, Goldberg HI, Hackney DB, Atlas SW, Kemp SS, Zimmerman RA, Bilaniuk LT. Mr imaging of hemorrhagic conditions of the head and neck. *Radiographics*. 1988;8:441-454
16. Goyal MS, Derdeyn CP. The diagnosis and management of supraaortic arterial dissections. *Curr Opin Neurol*. 2009;22:80-89
17. Georgiadis D, Arnold M, von Buedingen HC, Valko P, Sarikaya H, Rousson V, Mattle HP, Bousser MG, Baumgartner RW. Aspirin vs anticoagulation in carotid artery dissection: A study of 298 patients. *Neurology*. 2009;72:1810-1815
18. Lyrer P, Engelter S. Antithrombotic drugs for carotid artery dissection. *Cochrane Database Syst Rev*. 2010:CD000255
19. Edgell RC, Abou-Chebl A, Yadav JS. Endovascular management of spontaneous carotid artery dissection. *J Vasc Surg*. 2005;42:854-860; discussion 860
20. Schievink WI, Mokri B, O'Fallon WM. Recurrent spontaneous cervical-artery dissection. *N Engl J Med*. 1994;330:393-397
21. Dittrich R, Nassenstein I, Bachmann R, Maintz D, Nabavi DG, Heindel W, Kuhlenbaumer G, Ringelstein EB. Polyarterial clustered recurrence of cervical artery dissection seems to be the rule. *Neurology*. 2007;69:180-186
22. Touze E, Gauvrit JY, Moulin T, Meder JF, Bracard S, Mas JL. Risk of stroke and recurrent dissection after a cervical artery dissection: A multicenter study. *Neurology*. 2003;61:1347-1351
23. Oppenheim C, Naggara O, Touze E, Lacour JC, Schmitt E, Bonneville F, Crozier S, Guegan-Massardier E, Gerardin E, Leclerc X, Neau JP, Sirol M, Toussaint JF, Mas JL, Meder JF. High-resolution mr imaging of the cervical arterial wall: What the radiologist needs to know. *Radiographics*. 2009;29:1413-1431
24. Anzalone N, Scomazzoni F, Castellano R, Strada L, Righi C, Politi LS, Kirchin MA, Chiesa R, Scotti G. Carotid artery stenosis: Intraindividual correlations of 3d time-of-flight mr angiography, contrast-enhanced mr angiography, conventional dsa, and rotational angiography for detection and grading. *Radiology*. 2005;236:204-213
25. Kramer H, Runge VM, Morelli JN, Williams KD, Naul LG, Nikolaou K, Reiser MF, Wintersperger BJ. Magnetic resonance angiography of the carotid arteries: Comparison of unenhanced and contrast enhanced techniques. *Eur Radiol*. 2011;21:1667-1676
26. Saam T, Habs M, Cyran CC, Grimm J, Pfefferkorn T, Schuller U, Reiser MF, Nikolaou K. [new aspects of mri for diagnostics of large vessel vasculitis and primary angiitis of the central nervous system]. *Radiologe*. 2010;50:861-871
27. Naghavi M, Libby P, Falk E, Casscells SW, Litovsky S, Rumberger J, Badimon JJ, Stefanadis C, Moreno P, Pasterkamp G, Fayad Z, Stone PH, Waxman S, Raggi P, Madjid M, Zarrabi A, Burke A, Yuan C, Fitzgerald PJ, Siscovick DS, de Korte CL, Aikawa M,

- Juhani Airaksinen KE, Assmann G, Becker CR, Chesebro JH, Farb A, Galis ZS, Jackson C, Jang IK, Koenig W, Lodder RA, March K, Demirovic J, Navab M, Priori SG, Rekhater MD, Bahr R, Grundy SM, Mehran R, Colombo A, Boerwinkle E, Ballantyne C, Insull W, Jr., Schwartz RS, Vogel R, Serruys PW, Hansson GK, Faxon DP, Kaul S, Drexler H, Greenland P, Muller JE, Virmani R, Ridker PM, Zipes DP, Shah PK, Willerson JT. From vulnerable plaque to vulnerable patient: A call for new definitions and risk assessment strategies: Part i. *Circulation*. 2003;108:1664-1672
28. Chu B, Kampschulte A, Ferguson MS, Kerwin WS, Yarnykh VL, O'Brien KD, Polissar NL, Hatsukami TS, Yuan C. Hemorrhage in the atherosclerotic carotid plaque: A high-resolution mri study. *Stroke*. 2004;35:1079-1084
 29. Bley TA, Wieben O, Uhl M, Thiel J, Schmidt D, Langer M. High-resolution mri in giant cell arteritis: Imaging of the wall of the superficial temporal artery. *AJR Am J Roentgenol*. 2005;184:283-287
 30. Saam T, Raya JG, Cyran CC, Bochmann K, Meimarakis G, Dietrich O, Clevert DA, Frey U, Yuan C, Hatsukami TS, Werf A, Reiser MF, Nikolaou K. High resolution carotid black-blood 3t mr with parallel imaging and dedicated 4-channel surface coils. *J Cardiovasc Magn Reson*. 2009;11:41
 31. Zerizer I, Tan K, Khan S, Barwick T, Marzola MC, Rubello D, Al-Nahhas A. Role of fdg-pet and pet/ct in the diagnosis and management of vasculitis. *Eur J Radiol*. 2010;73:504-509
 32. Blockmans D, De Ceuninck L, Vanderschueren S, Knockaert D, Mortelmans L, Bobbaers H. Repetitive 18-fluorodeoxyglucose positron emission tomography in isolated polymyalgia rheumatica: A prospective study in 35 patients. *Rheumatology (Oxford)*. 2007;46:672-677
 33. Meller J, Strutz F, Siefker U, Scheel A, Sahlmann CO, Lehmann K, Conrad M, Vosschenrich R. Early diagnosis and follow-up of aortitis with [(18)f]fdg pet and mri. *Eur J Nucl Med Mol Imaging*. 2003;30:730-736
 34. Tezuka D, Haraguchi G, Ishihara T, Ohigashi H, Inagaki H, Suzuki J, Hirao K, Isobe M. Role of fdg pet-ct in takayasu arteritis: Sensitive detection of recurrences. *JACC Cardiovasc Imaging*. 2012;5:422-429
 35. Rominger A, Saam T, Wolpers S, Cyran CC, Schmidt M, Foerster S, Nikolaou K, Reiser MF, Bartenstein P, Hacker M. 18f-fdg pet/ct identifies patients at risk for future vascular events in an otherwise asymptomatic cohort with neoplastic disease. *J Nucl Med*. 2009;50:1611-1620
 36. Kim TN, Kim S, Yang SJ, Yoo HJ, Seo JA, Kim SG, Kim NH, Baik SH, Choi DS, Choi KM. Vascular inflammation in patients with impaired glucose tolerance and type 2 diabetes: Analysis with 18f-fluorodeoxyglucose positron emission tomography. *Circ Cardiovasc Imaging*. 2010;3:142-148

37. Tahara N, Kai H, Yamagishi S, Mizoguchi M, Nakaura H, Ishibashi M, Kaida H, Baba K, Hayabuchi N, Imaizumi T. Vascular inflammation evaluated by [18f]-fluorodeoxyglucose positron emission tomography is associated with the metabolic syndrome. *J Am Coll Cardiol*. 2007;49:1533-1539
38. Kwee RM, Teule GJ, van Oostenbrugge RJ, Mess WH, Prins MH, van der Geest RJ, Ter Berg JW, Franke CL, Korten AG, Meems BJ, Hofman PA, van Engelshoven JM, Wildberger JE, Kooi ME. Multimodality imaging of carotid artery plaques: 18f-fluoro-2-deoxyglucose positron emission tomography, computed tomography, and magnetic resonance imaging. *Stroke*. 2009;40:3718-3724
39. Silvera SS, Aidi HE, Rudd JH, Mani V, Yang L, Farkouh M, Fuster V, Fayad ZA. Multimodality imaging of atherosclerotic plaque activity and composition using fdg-pet/ct and mri in carotid and femoral arteries. *Atherosclerosis*. 2009;207:139-143
40. Brix G, Lechel U, Glatting G, Ziegler SI, Munzing W, Muller SP, Beyer T. Radiation exposure of patients undergoing whole-body dual-modality 18f-fdg pet/ct examinations. *J Nucl Med*. 2005;46:608-613
41. Forster K, Poppert H, Conrad B, Sander D. Elevated inflammatory laboratory parameters in spontaneous cervical artery dissection as compared to traumatic dissection: A retrospective case-control study. *J Neurol*. 2006;253:741-745
42. Volker W, Besselmann M, Dittrich R, Nabavi D, Konrad C, Dziewas R, Evers S, Grewe S, Kramer SC, Bachmann R, Stogbauer F, Ringelstein EB, Kuhlenbaumer G. Generalized arteriopathy in patients with cervical artery dissection. *Neurology*. 2005;64:1508-1513
43. Lusby RJ, Ferrell LD, Ehrenfeld WK, Stoney RJ, Wylie EJ. Carotid plaque hemorrhage. Its role in production of cerebral ischemia. *Arch Surg*. 1982;117:1479-1488
44. Goldberg HI, Grossman RI, Gomori JM, Asbury AK, Bilaniuk LT, Zimmerman RA. Cervical internal carotid artery dissecting hemorrhage: Diagnosis using mr. *Radiology*. 1986;158:157-161

2. ERGEBNISSE

2.1. Vessel Wall Inflammation in Spontaneous Cervical Artery Dissection:

A Prospective, Observational Positron Emission Tomography, Computed Tomography, and Magnetic Resonance Imaging Study

Thomas Pfefferkorn, Tobias Saam, Axel Rominger, Maximilian Habs, Lisa-Ann Gerdes, Caroline Schmidt, Clemens Cyran, Andreas Straube, Jennifer Linn, Konstantin Nikolaou, Peter Bartenstein, Maximilian Reiser, Marcus Hacker, Martin Dichgans

Stroke. 2011 Jun;42(6):1563-8. Epub 2011 Apr 21.

2.2. Age determination of vessel wall hematoma in spontaneous cervical artery dissection:

A multi-sequence 3T Cardiovascular Magnetic Resonance Study

Maximilian Habs, Thomas Pfefferkorn, Clemens Cyran, Jochen Grimm, Axel Rominger, Marcus Hacker, Christian Opherk, Maximilian Reiser, Konstantin Nikolaou, Tobias Saam

J Cardiovasc Magn Reson. 2011 Nov 28;13(1):76.
(Epub ahead of print)

Vessel Wall Inflammation in Spontaneous Cervical Artery Dissection

A Prospective, Observational Positron Emission Tomography, Computed Tomography, and Magnetic Resonance Imaging Study

Thomas Pfefferkorn, MD; Tobias Saam, MD; Axel Rominger, MD; Maximilian Habs; Lisa-Ann Gerdes, MD; Caroline Schmidt, MD; Clemens Cyran, MD; Andreas Straube, MD; Jennifer Linn, MD; Konstantin Nikolaou, MD; Peter Bartenstein, MD; Maximilian Reiser, MD; Marcus Hacker, MD; Martin Dichgans, MD

Author Affiliations

From the Department of Neurology (T.P., L.A.G., C.S., A.S., M.S.),
Department of Clinical Radiology (T.S., M.H., C.C., K.N., M.R.),
Department of Nuclear Medicine (A.R., P.B., M.H.),
Department of Neuroradiology (J.L.), and
Institute for Stroke and Dementia Research (M.D.)

Klinikum Grosshadern, University of Munich, Munich, Germany

Correspondence

Thomas Pfefferkorn, MD,
Department of Neurology, Klinikum Grosshadern
University of Munich
Marchioninistrasse 15
81377 Munich
Germany
E-mail: Thomas.Pfefferkorn@med.uni-muenchen.de

Abstract

Background and Purpose: Vessel wall inflammation (VWI) may be a pathogenetic factor in cervical artery dissection (CAD). We used contrast-enhanced high-resolution MRI (hrMRI) and positron emission tomography CT (PET-CT) to systematically investigate VWI in spontaneous CAD.

Methods: In this monocentric, prospective, observational study, all consecutive patients with acute, MRI-confirmed, spontaneous CAD admitted to our center between August 2007 and August 2009 were included. VWI was defined as perivascular contrast enhancement in hrMRI and increased perivascular [18F]-fluorodesoxyglucose uptake in PET-CT. VWI was further differentiated between local (restricted to the site of dissection) and generalized (exceeding the site of dissection).

Results: A total of 37 patients were included. Multiple dissections were seen in 10 patients (27%). Twenty-five patients received both modalities as planned, 8 received only PET-CT, and 4 received only hrMRI. A subset of patients showed signs of a generalized VWI in hrMRI (4/29 patients, 14%) and PET-CT (8/33 patients, 24%). In patients who received both modalities, all with hrMRI signs of generalized VWI were PET-CT positive (3/3), whereas some PET-CT-positive patients were hrMRI-negative (4/7). If present, generalized VWI in hrMRI completely resolved within 6 months. The presence of >2 simultaneous dissections (seen in 2 patients) was significantly associated with generalized VWI in hrMRI ($P=0.015$) but marginally not in PET-CT ($P=0.053$).

Conclusions: A subset of patients with spontaneous CAD showed signs of a generalized transient inflammatory arteriopathy in contrast-enhanced hrMRI and PET-CT. This subset of patients may be more prone to multiple dissections.

Key Words: cervical artery dissection – inflammation – positron emission tomography

Background

Cervical artery dissection (CAD) is a relevant cause of stroke in younger patients. Its pathophysiology is poorly understood. Possible constitutional factors include connective tissue disorders¹ and genetic predisposition.² Environmental factors include major³ and minor^{4,5} trauma but also recent infection.^{6,7} A possible causal role of recent infection is supported by a seasonal peak of CAD in autumn.⁸ Consistent with that, several studies have demonstrated elevated serum markers of inflammation in patients with CAD.^{9,10} Furthermore, evidence for a generalized arteriopathy in spontaneous CAD patients has been previously provided by microscopic signs of tissue weakening in biopsy specimens of the superficial temporal artery.¹¹

Modern imaging modalities are capable to demonstrate vessel wall inflammation. Specifically, [18F]-fluorodesoxyglucose positron emission tomography CT (PET-CT) is able to detect large vessel inflammation with high sensitivity¹² and may be used to predict the risk of unfavorable outcome in acute aortic dissection.¹³ Moreover, PET-CT and MRI are increasingly used to image atherosclerotic plaque inflammation and morphology.^{14,-,16} High-resolution MRI (hrMRI) recently has been applied to characterize cervical and intracranial artery pathology, including inflammatory vessel wall alterations.^{17,18} In another recent study, hrMRI demonstrated increased periarterial edema in spontaneous compared to traumatic CAD.¹⁹ To further elucidate the role of vessel wall inflammation (VWI) in spontaneous CAD, we performed a monocentric, prospective, observational rater-blinded PET-CT and hrMRI study focusing on perivascular [18F]-fluorodesoxyglucose uptake (PET-CT), perivascular contrast enhancement (hrMRI), and perivascular edema (hrMRI).

Patients and Methods

Patients

All consecutive patients with the first manifestation of spontaneous cervical artery dissection treated at our center between August 2007 and August 2009 were included in the study if the following inclusion criteria were fulfilled: (1) unequivocal MRI evidence of cervical artery dissection (hyperintense signal in fat-suppressed T1 sequences demonstrating intramural met hemoglobin); (2) written informed consent; and (3) admission at our center within 4 weeks after symptom onset, which enabled us to perform PET-CT and hrMRI within 5 weeks. The date of dissection was estimated from the first appearance of ≥ 1 of the following symptoms or signs: acute cervical pain; local symptoms such as cervical swelling or Horner syndrome; and clinical features of cerebral ischemia. Patients with a history of a related trauma, a preexisting diagnosis of arteritis, or an underlying disease clearly associated with CAD were excluded. Standard diagnostic procedures included laboratory investigations for markers of inflammation (C-reactive protein on admission) and extracranial and intracranial Duplex sonography. VWI was assessed by hrMRI and PET-CT as described. All patients were seen 3 to 6 months after the initial presentation for a clinical and sonographic follow-up. If patients showed signs of a generalized VWI in the initial hrMRI, then a second hrMRI investigation was performed at follow-up. The study was approved by the local institutional Ethics Committee and complied with the declaration of Helsinki.

MRI

Patients underwent hrMRI at 3.0 T (Magnetom Verio; Siemens Healthcare). Sequences included fat-suppressed and blood-suppressed T1 sequences with and without contrast agent, T2 sequences, and time of flight angiography. To improve signal-to-noise performance and optimize spatial resolution, a dedicated four-channel surface coil (Machnet, Eelde, Netherlands) for bilateral carotid scans was used in combination with the head and neck coil. All patients obtained a multi-sequence protocol without ECG gating or motion correction using Parallel Imaging techniques (PAT factor = 2). The protocol included a fat- and blood suppressed 2D-T1 Turbo Spin Echo (TSE) sequence [TR=800 ms, TE=12 ms, Field of View (FOV)=160 x 120 mm] with and without contrast agent [intravenous injection of 0.1 mmol/kg Gadobutrol (Gadovist®, Bayer Schering, Leverkusen, Germany)], a fat- and blood suppressed 2D-T2 TSE sequence (TR=3000

ms, TE=65 ms, FOV=160 x 120 mm) and a 3D-GRE time-of-flight angiography (TOF; TR=21 ms, TE=3.96 ms, FOV=160 x 120 mm). Best in plane resolution was 0.5 x 0.5 mm² with a slice thickness of 4 mm for T1- and T2- weighted images and 1 mm for TOF images. Number of slices was 20 – 30 for T1-, 24-36 for T2- and 104 for TOF images. Total scan time was on average 35 minutes. Coverage reached from the shoulders to the base of the skull. Therefore, contrast enhancement in the common carotid arteries, internal carotid arteries, external carotid arteries, and vertebral arteries could be analyzed. Off-line, 2 experienced radiologists blinded to clinical and PET-CT data rated contrast enhancement (yes/no) and perivascular edema (yes/no). If contrast enhancement was restricted to the site of the dissection, then this alteration was rated as local VWI. If it was observed not only in the dissected but also in any other not dissected artery, then it was rated as generalized VWI.

PET-CT

PET-CT studies were performed on 2 different scanners. Initially, the PET-CT scanner Philips Gemini (Philips Healthcare) was used, which was substituted during the study by the Siemens Biograph 64 (Siemens Healthcare). Patients fasted for 6h to ensure a blood glucose level below 130mg/ml. Five MBq of [18F]-FDG per kg body weight were injected one hour before scanning. The patients rested in a comfortable sitting position and then were brought to the scanning suite. First, transmission data were acquired by means of a low-dose CT scan (20 mAs, 140kV, 512 x 512 matrix, 6-mm slice thickness, increment of 5 mm/s, rotation time of 0.5 s, pitch index of 1.5). PET emission scans were acquired afterwards in caudocephalad direction in 3D-mode with a 144 x 144 matrix. After scatter and decay-correction, PET data were reconstructed iteratively with and without attenuation correction and then reoriented in axial, sagittal and coronal slices with a slice thickness of 4 mm (Philips scanner) and 5 mm (Siemens scanner) respectively, yielding a spatial resolution of 6 mm.. Coverage reached from the diaphragm to the base of the skull. Off-line, 2 experienced reviewers blinded to clinical and hrMRI data rated increased perivascular glucose metabolism (yes/no). If these alterations were restricted to the site of the dissection, then they were rated as local VWI. If the alterations were observed not only in the dissected but also in any other artery not dissected, then they were rated as generalized VWI. Additionally, standardized uptake values were quantified in the aorta and both carotid and both vertebral arteries. From these, target-to-blood pool ratios (TBR) were derived (arterial standardized uptake values_{max}/venous standardized uptake values_{mean}).²⁰ These can be reproducibly obtained scanner-

independently.²¹ To match the PET-CT and MR images, we used several landmarks, such as the carotid bifurcation, the further course of the carotid and vertebral arteries, and the vertebral bodies. All these structures clearly can be identified both on MR and PET-CT images.

Statistical Analysis

Values are given as mean±SD. Groups were compared by univariate analysis using the independent t test for comparison of continuous variables and the Fisher exact test for comparison of proportions. Because of the relatively low number of patients, we did not perform a logistic regression analysis.

Results

Patients Characteristics

A total of 44 patients were screened. Seven of them were not enrolled in the study because of delayed presentation (>35 days). Basic data of the 37 enrolled patients are presented in the [Table](#). In 4 patients, PET-CT was not performed because of withdrawn consent after the MRI examination. In 8 patients, MRI was not performed because of logistical problems at the beginning of the study. This resulted in 25 patients who received both modalities. Eight patients only had PET-CT and 4 had only hrMRI performed. All patients received standard therapy with heparin, which was later switched to oral anticoagulation (phenprocoumon; international normalized ratio, 2.0–3.0) for at least 6 months. No patient had a CAD or stroke recurrence within 6 months after the initial presentation. Thirty-four patients (92%) had a good functional outcome after 6 months, defined as a modified Rankin scale score of ≤ 2 .

Affected Arteries and Clinical Manifestations

A total of 49 cervical artery dissections (30 carotid and 19 vertebral artery dissections) were detected in the 37 patients. In 10 patients (27%), multiple arteries were affected; in 2 patients (5%), 3 arteries were affected. Most patients presented with signs of cerebral ischemia (TIA, 14%; stroke, 54%). A minority of patients (32%) only showed local symptoms such as cervical pain or Horner syndrome.

MRI and PET-CT Findings

In the majority of patients (27/33; 82%), PET-CT showed increased [18F]-fluorodesoxyglucose accumulation at the site of the dissection ([Figures 1–3](#)). In a limited number of patients (8/33; 24%), these alterations exceeded the site of the dissection ([Figures 1, 2](#)), suggesting generalized VWI.

A similar pattern was observed with hrMRI. In the majority of patients (21/29; 72%), perivascular contrast enhancement was found at the site of the dissection ([Figures 2, 3](#)). And, again, in a limited number of patients (4/29; 14%), perivascular contrast enhancement exceeded the site of the dissection ([Figure 2](#)). Perivascular edema at the site of the dissection was observed in approximately half of the patients (15/29; 52%). It exceeded the site of the dissection in the same 4 patients who showed generalized contrast enhancement (4/29; 14%; [Figure 2](#)). In these 4

patients, control hrMRI 3 to 6 months later showed complete resolution of contrast enhancement and perivascular edema (Figure 4). Intramural hematoma also regressed over time (Supplemental Figure S1).

All patients with hrMRI signs of generalized VWI (3/3) also had PET-CT signs of generalized VWI, whereas 4 out of 7 PET-CT-positive patients were hrMRI-negative. In 3 of these 4 patients, generalized VWI in PET-CT was deducted from increased [18F]-fluorodesoxyglucose uptake in the aortic arch, a region that was not captured by hrMRI. This left only 1 patient in whom PET-CT and hrMRI provided conflicting results with regard to generalized VWI.

Quantitative PET-CT analyses revealed higher mean TBR values in dissected than in nondissected arteries (1.48 ± 0.56 versus 1.12 ± 0.25 ; $P < 0.001$; Figure 5A). Patients with multiple dissections tended to have higher mean TBR values in the (never dissected) aortic arch (1.55 ± 0.20 versus 1.41 ± 0.20 ; $P = 0.08$; Figure 5B). Mean TBR values were also increased in arteries in which hrMRI had demonstrated perivascular contrast enhancement (1.58 ± 0.64 versus 1.13 ± 0.27 ; $P < 0.001$; Figure 5C) or perivascular edema (1.56 ± 0.64 versus 1.16 ± 0.33 ; $P < 0.001$; Figure 5D).

In univariate analysis, generalized VWI in PET-CT was associated with younger age (Table). Patients with multiple dissections tended to more often show signs of generalized VWI in hrMRI and PET-CT; however, these trends were not statistically significant (Table). The presence of >2 dissections (seen in 2 patients) was significantly associated with signs of generalized VWI in hrMRI but marginally not in PET-CT (Table). Mean C-reactive protein values on admission tended to be higher in patients with signs of generalized VWI in hrMRI and PET-CT, yet these trends were not statistically significant (Table).

Discussion

In our prospective observational imaging study, local signs of VWI were a frequent finding in patients with spontaneous CAD. However, in approximately one-fifth of our patients, signs of VWI exceeded the site of CAD, suggesting a generalized inflammatory arteriopathy.

In the absence of histopathology, one may question whether the observed hrMRI and PET-CT alterations really demonstrate VWI. The concept of an underlying inflammation, however, is strongly supported by the fact that our 4 patients with generalized perivascular contrast enhancement also showed generalized perivascular edema in hrMRI and (if examined) generalized increased [18F]-fluorodesoxyglucose uptake in PET-CT. An underlying transient inflammatory process is further supported by the observation that these generalized vessel wall alterations (detected by hrMRI) resolved within weeks. It is important to note that time intervals from symptom onset to hrMRI and PET-CT were similar in patients with and without signs of generalized VWI. This argues against the conception that the observed hrMRI and PET-CT findings may be a regular time-dependent feature of CAD.

An underlying transient inflammatory arteriopathy may explain the frequently observed occurrence of multiple dissections at 1 point in time and the relatively low risk of late CAD recurrence in affected patients.^{22,23} In our study, more than one-quarter of patients were affected by multiple dissections. These patients tended to have higher mean TBR values in the (not dissected) aortic arch than those with only 1 dissection. They also tended to more often show signs of generalized VWI in PET-CT and hrMRI. Interestingly, the presence of >2 dissections, as seen in 2 of our patients, was in fact significantly associated with signs of generalized VWI in hrMRI. These findings support the idea of an inflammatory pathogenetic factor in a subset of CAD patients.

Our study may have been underpowered to demonstrate an association between signs of generalized VWI and serum markers of inflammation. We can only provide trends for higher C-reactive protein values in patients with signs of generalized VWI. This finding should be tested in larger patient populations.

Arteries showing contrast enhancement or perivascular edema in hrMRI had higher TBR values in PET-CT, suggesting that both methods can be used to assess VWI. The observed higher

rate of generalized VWI in PET-CT compared to hrMRI may, in part, be explained by the additional PET-CT assessment of the aortic arch, which could not be covered by hrMRI. Surprisingly, signs of generalized VWI in PET-CT were associated with younger age. The hrMRI did not demonstrate a similar association. This may be explained by a decreasing sensitivity of PET-CT with age caused by a higher atherosclerosis-related background activity in older individuals.¹⁵

Because of the good functional outcome in most of our patients, we cannot provide much information on the clinical, therapeutic, and prognostic relevance of generalized VWI in CAD. Because the hrMRI signs of generalized VWI resolved in all affected patients within a few months, long-term consequences may not arise. However, it remains unclear whether affected CAD patients may benefit from short-term anti-inflammatory or antibiotic therapy. Only trials much larger than ours could possibly answer this question. Because MRI is increasingly used in the routine diagnostic work-up of CAD patients,²⁴ high-resolution, contrast-enhanced, T1-weighted sequences easily could be included in a respective study protocol.

Conclusions

In conclusion, a subset of patients with spontaneous CAD showed signs of a generalized transient inflammatory arteriopathy in PET-CT and contrast enhanced hrMRI. This subset of patients may be more prone to multiple dissections. Multicenter efforts are needed to confirm our findings in larger patient populations.

Disclosure

None.

Acknowledgments

The authors thank K. Ogston for language editing of the manuscript.

References

1. Brandt T, Hausser I, Orberk E, Grau A, Hartschuh W, Anton-Lamprecht I, Hacke W. Ultrastructural connective tissue abnormalities in patients with spontaneous cervicocerebral artery dissections. **Ann Neurol.** 1998; 44: 281–285.
2. Debette S, Markus HS. The genetics of cervical artery dissection: a systematic review. **Stroke.** 2009; 40: e459–e466.
3. Biffi WL, Ray CE Jr., Moore EE, Franciose RJ, Aly S, Heyrosa MG, Johnson JL, Burch JM. Treatment-related outcomes from blunt cerebrovascular injuries: importance of routine follow-up arteriography. **Ann Surg.** 2002; 235: 699–706.
4. Dittrich R, Rohsbach D, Heidbreder A, Heuschmann P, Nassenstein I, Bachmann R, Ringelstein EB, Kuhlenbäumer G, Nabavi DG. Mild mechanical traumas are possible risk factors for cervical artery dissection. **Cerebrovasc Dis.** 2007; 23: 275–281.
5. Haldeman S, Kohlbeck FJ, McGregor M. Stroke, cerebral artery dissection, and cervical spine manipulation therapy. **J Neurol.** 2002; 249: 1098–1104.
6. Grau AJ, Brandt T, Buggle F, Orberk E, Mytilineos J, Werle E, Conradt, Krause M, Winter R, Hacke W. Association of cervical artery dissection with recent infection. **Arch Neurol.** 1999; 56: 851–856.
7. Guillon B, Berthet K, Benslamia L, Bertrand M, Boussier MG, Tzourio C. Infection and the risk of spontaneous cervical artery dissection: a case-control study. **Stroke.** 2003; 34: e79–e81.
8. Schievink WI, Wijdicks EF, Kuiper JD. Seasonal pattern of spontaneous cervical artery dissection. **J Neurosurg.** 1998; 89: 101–103.
9. Forster K, Poppert H, Conrad B, Sander D. Elevated inflammatory laboratory parameters

- in spontaneous cervical artery dissection as compared to traumatic dissection: a retrospective case-control study. **J Neurol.** 2006; 253: 741–745.
10. Genius J, Dong-Si T, Grau AP, Lichy C. Postacute C-reactive protein levels are elevated in cervical artery dissection. **Stroke.** 2005; 36: e42–e44.
 11. Völker W, Besselmann M, Dittrich R, Nabavi D, Konrad C, Dziewas R, Evers S, Grewe S, Krämer SC, Bachmann R, Stögbauer F, Ringelstein EB, Kuhlenbäumer G. Generalized arteriopathy in patients with cervical artery dissection. **Neurology.** 2005; 64: 1508–1513.
 12. Pipitone N, Versari A, Salvarani C. Role of imaging studies in the diagnosis and follow-up of large-vessel vasculitis: an update. **Rheumatology (Oxford).** 2008; 47: 403–408.
 13. Kato K, Nishio A, Kato N, Usami H, Fujimaki T, Murohara T. Uptake of 18F-FDG in acute aortic dissection: a determinant of unfavorable outcome. **J Nucl Med.** 2010; 51: 674–681.
 14. Kwee RM, Teule GJ, van Oostenbrugge RJ, Mess WH, Prins MH, van der Geest RJ, Ter Berg JW, Franke CL, Korten AG, Meems BJ, Hofman PA, van Engelshoven JM, Wildberger JE, Kooi ME. Multimodality imaging of carotid artery plaques: 18F-fluoro-2-deoxyglucose positron emission tomography, computed tomography, and magnetic resonance imaging. **Stroke.** 2009; 40: 3718–3724.
 15. Rudd JH, Narula J, Strauss HW, Virmani R, Machac J, Klimas M, Tahara N, Fuster V, Warburton EA, Fayad ZA, Tawakol AA. Imaging atherosclerotic plaque inflammation by fluorodeoxyglucose with positron emission tomography: ready for prime time? **J Am Coll Cardiol.** 2010; 55: 2527–2535.
 16. Rudd JH, Myers KS, Bansilal S, Machac J, Pinto CA, Tong C, Rafique A, Hargeaves R, Farkouh M, Fuster V, Fayad ZA. Atherosclerosis inflammation imaging with 18F-FDG PET: carotid, iliac, and femoral uptake reproducibility, quantification methods, and recommendations. **J Nucl Med.** 2008; 49: 871–878.

17. Küker W, Gaertner S, Nagele T, Dopfer C, Schoning M, Fiehler J, Rothwell PM, Herrlinger U. Vessel wall contrast enhancement: a diagnostic sign of cerebral vasculitis. **Cerebrovasc Dis.** 2008; 26: 23–29.
18. Saam T, Raya JG, Cyran CC, Bochmann K, Meimarakis G, Dietrich O, Clevert DA, Frey U, Yuan C, Hatsukami TS, Werf A, Reiser MF, Nikolaou K. High resolution carotid black-blood 3T MR with parallel imaging and dedicated 4-channel surface coils. **J Cardiovasc Magn Reson.** 2009; 11: 41.
19. Naggara O, Touzé E, Marsico R, Leclerc X, Nguyen T, Mas JL, Pruvo JP, Meder JF, Oppenheim C. High-resolution MR imaging of periarterial edema associated with biological inflammation in spontaneous carotid dissection. **Eur Radiol.** 2009; 19: 2255–2260.
20. Rominger A, Saam T, Wolpers S, Cyran CC, Schmidt M, Foerster S, Nikolaou K, Reiser MF, Bartenstein P, Hacker M. 18F-FDG PET/CT identifies patients at risk for future vascular events in an otherwise asymptomatic cohort with neoplastic disease. **J Nucl Med.** 2009; 50: 1611–1620.
21. Rominger A, Rist C, Nikolaou K, Reiser MF, Bartenstein P, Hacker M, Saam T. [PET/CT imaging of atherosclerotic blood vessel alterations]. **Radiologe.** 2010; 50: 355–365.
22. Lee VH, Brown RD Jr., Mandrekar JN, Mokri B. Incidence and outcome of cervical artery dissection: a population-based study. **Neurology.** 2006; 67: 1809–1812.
23. Touzé E, Gauvrit JY, Moulin T, Meder JF, Bracard S, Mas JL. Multicenter Survey on Natural History of Cervical Artery Dissection. Risk of stroke and recurrent dissection after a cervical artery dissection: a multicenter study. **Neurology.** 2003; 61: 1347–1351.
24. Debette S, Leys D. Cervical-artery dissections: predisposing factors, diagnosis, and outcome. **Lancet Neurol.** 2009; 8: 668–678.

Table.							
Patient Characteristics With (+) and Without (–) Signs of Generalized Vessel Wall Inflammation in High-Resolution Magnetic Resonance Imaging and Positron Emission Tomography Computed Tomography							
	All (n=37)	hrMRI– (n=25)	hrMRI+ (n=4)	P	PET–CT– (n=25)	PET–CT+ (n=8)	P
Age (y)	43±9	44±9	40±16	0.479	45±8	36±8	0.011
Female	38%	32%	75%	0.139	32%	63%	0.213
Active smoking	36%	40%	25%	1.000	38%	25%	0.675
Arterial hypertension	34%	33%	25%	1.000	45%	25%	0.419
Hypercholesterolemia	22%	25%	25%	1.000	30%	0%	0.141
Time to MRI (d)*	14±9	14±9	14±10	0.950	NA	NA	NA
Time to PET–CT (d)*	18±10	NA	NA	NA	16±10	22±9	0.135
CRP on admission (mg/dL)	0.43±0.39	0.42±0.38	0.85±0.57	0.059	0.37±0.31	0.53±0.51	0.309
>1 dissection	27%	24%	50%	0.300	20%	50%	0.170
>2 dissections	5%	0%	50%	0.015	0%	25%	0.053

- CRP indicates C-reactive protein; CT, computed tomography; hrMRI, high-resolution magnetic resonance imaging; MRI, magnetic resonance imaging; NA, not available; PET, positron emission tomography.

^{*} From symptom onset.

Figure legends

Figure 1: Multiple cervical artery dissections in a 41-year-old woman (imaging 1 week after symptom onset). MR angiography (A) shows dissections of the left internal carotid artery (arrow) and both vertebral arteries (double arrow). Axial computed tomography (CT) (B), positron emission tomography (PET) (C), and PET-CT (D) images show pathological [18F]-fluorodesoxyglucose uptake of the aortic arch, particularly at the origin of the supra-aortic vessels (arrows). MRA indicates magnetic resonance angiography.

Figure 2: Axial fat-suppressed black-blood precontrast and postcontrast T1-weighted images (A, B), T2-weighted images (C) and positron emission tomography CT images (D) of the cervical arteries of the same patient as in Figure 1. The chevron in (A) points to the intramural vessel wall hematoma/arterial dissection of the left internal carotid artery. The inflammatory changes are not confined to the site of the arterial dissection; both carotid arteries demonstrate pathological [18F]-fluorodesoxyglucose uptake (black arrows in D). MRI images show perivascular contrast enhancement (B) and perivascular edema (C) of both carotid arteries (white arrows), consistent with vessel wall inflammation. The dotted arrows in (B) point to the vertebral arteries, which show a slightly increased perivascular contrast enhancement. CE indicates contrast enhancement; PET, positron emission tomography; CT, computed tomography.

Figure 3: Axial fat-suppressed black-blood precontrast and postcontrast T1-weighted images (A, B), T2-weighted images (C), and positron emission tomography CT images (D) of the vertebral arteries of a 48-year-old patient with left-side vertebral artery dissection (imaging 3 weeks after symptom onset). A, Weak hyperintense signal (arrow) on precontrast T1-weighted imaging demonstrating left vertebral artery dissection. B, Perivascular contrast enhancement of the left vertebral artery. Of note, no contrast enhancement is seen in the right vertebral artery, confirming that local vessel wall inflammation was confined to the site of the arterial dissection. C, Local perivascular edema. D, Pathological [18F]-fluorodesoxyglucose uptake at the site of the dissection. CE indicates contrast enhancement; PET, positron emission tomography; CT, computed tomography.

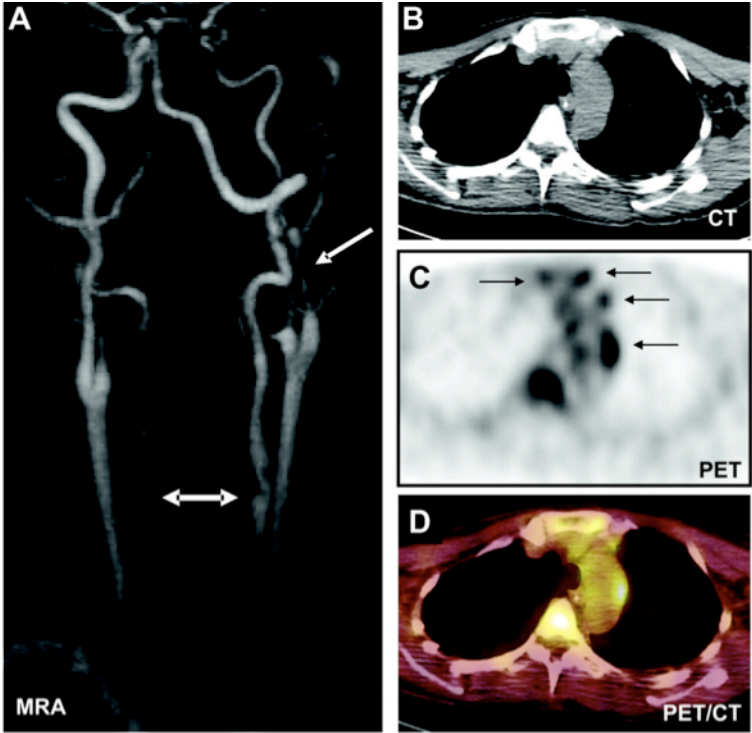
Figure 4: Axial MR images in black-blood technique of the same patient as in Figures 1 and 2 at baseline (A, B) and 4 months later (C, D). The arrows in (A) and (B) point to areas of perivascular contrast enhancement and edema in both internal carotid arteries, consistent with

vessel wall inflammation. At follow-up (C, D), the inflammatory changes had completely resolved. CE indicates contrast enhancement.

Figure 5: Mean target-to-blood pool ratios (TBR) of [18F]-fluorodesoxyglucose uptake measured by positron emission tomography CT. A, Increased TBR values in dissected compared to normal arteries. B, Nonsignificant trend for increased TBR values in the aortic arch in patients with multiple dissections compared to patients with a single dissection. C, Increased TBR values in arteries with compared to arteries without perivascular contrast enhancement (CE) in high-resolution MRI. D, Increased TBR values in arteries with compared to arteries without perivascular edema (PVE) in high-resolution MRI. Error bars indicate standard deviation.

Figure S1: Resolution of intramural hematoma over time. Axial MR images in a patient with left carotid artery dissection (arrows). Time of flight (TOF) angiography and T1 demonstrate typical lumen narrowing (A) and intramural hematoma (B) in the acute phase. Four months later these alterations have regressed (C, D). Additional images of the same patient are presented in the manuscript (Figures 2 and 4).

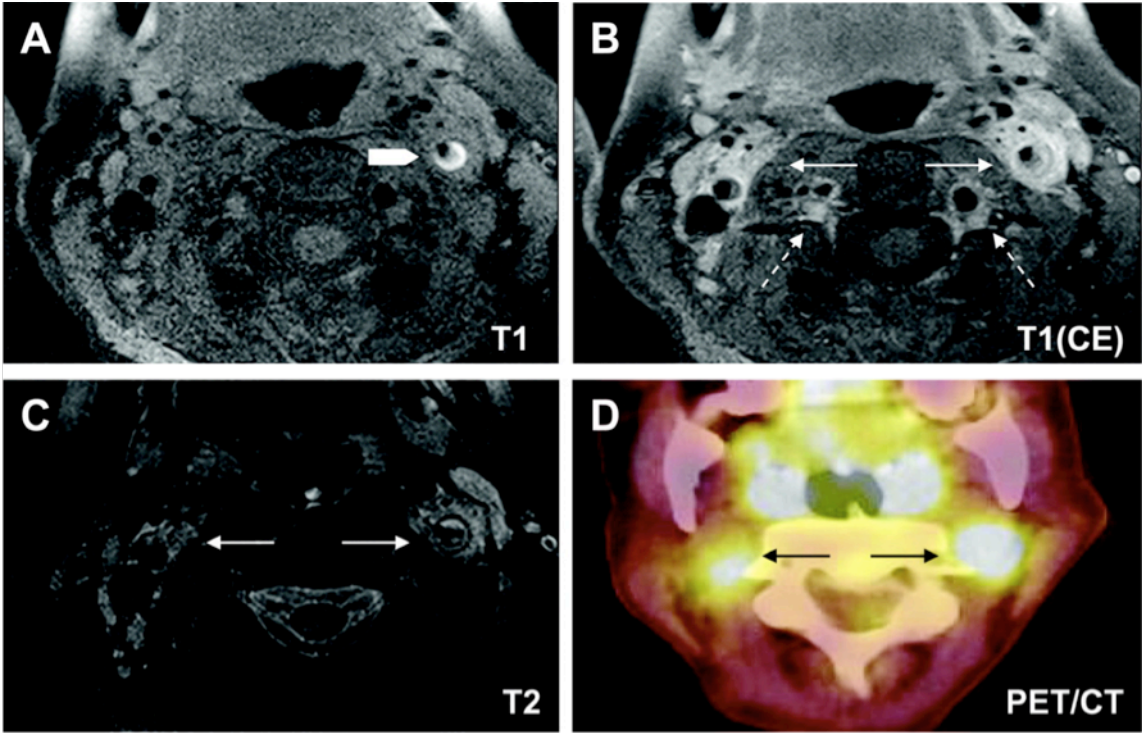
Figure 1



Pfefferkorn T et al. Stroke 2011;42:1563-1568

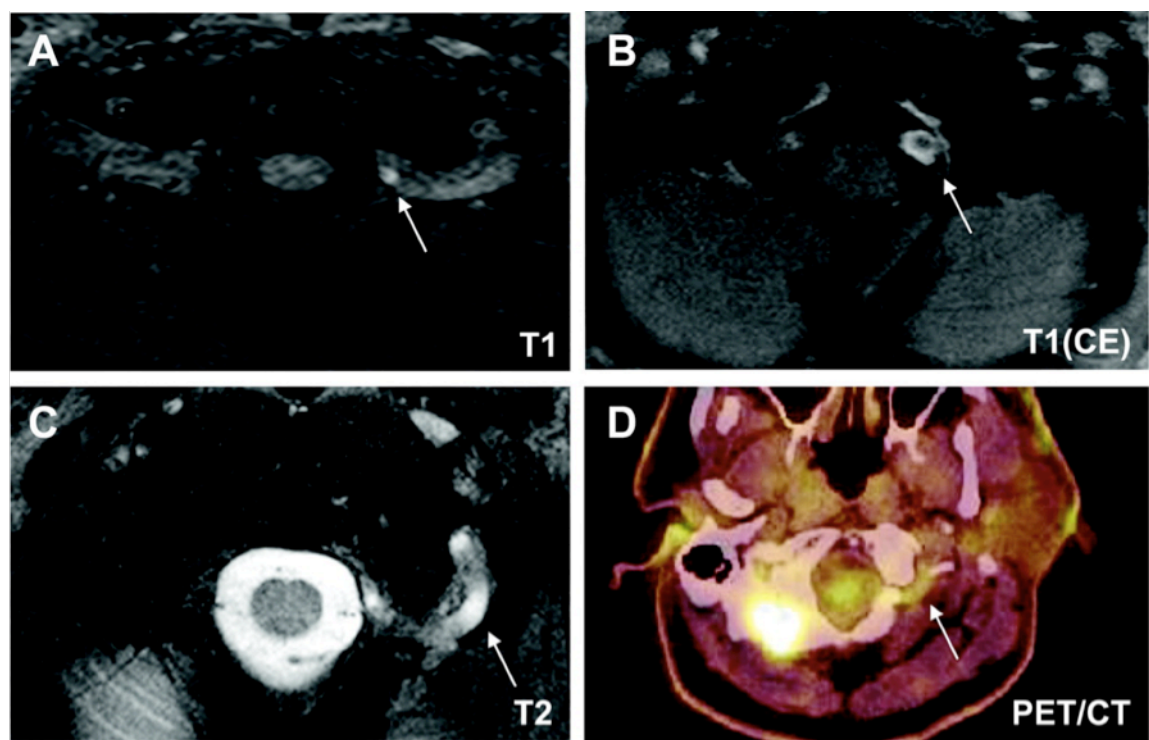
Copyright © American Heart Association

Figure 2




Pfefferkorn T et al. Stroke 2011;42:1563-1568

Figure 3

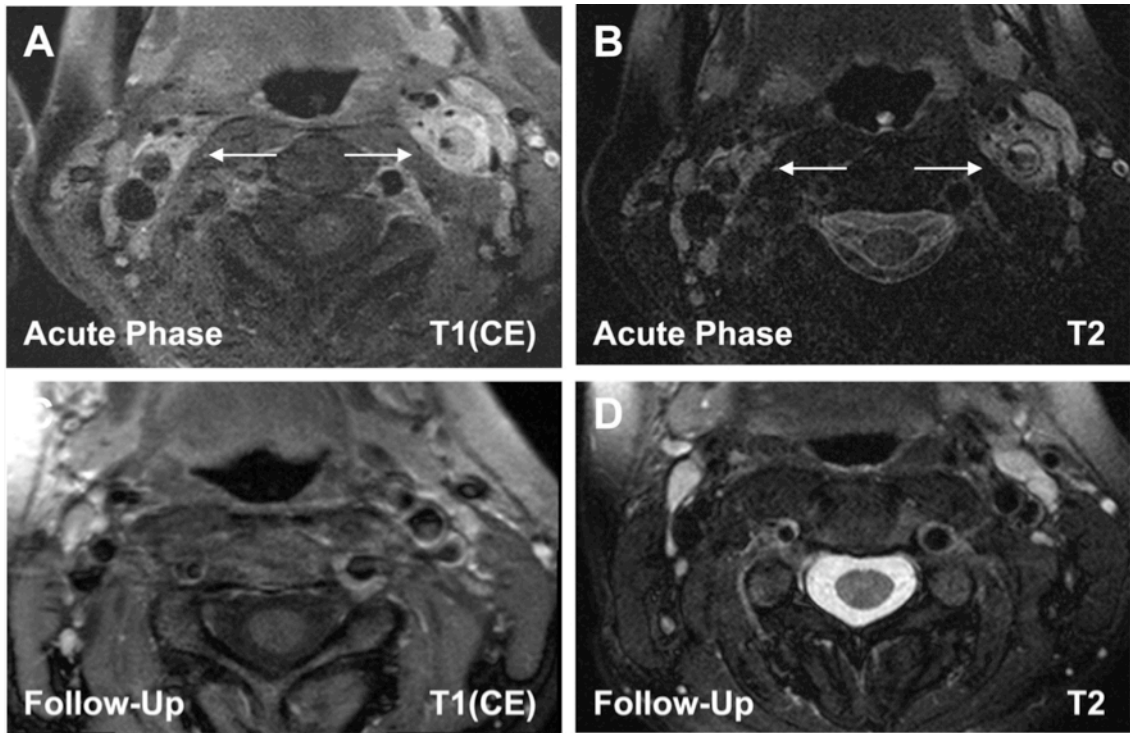


Pfefferkorn T et al. Stroke 2011;42:1563-1568

American Heart Association 
Learn and Live

Copyright © American Heart Association

Figure 4

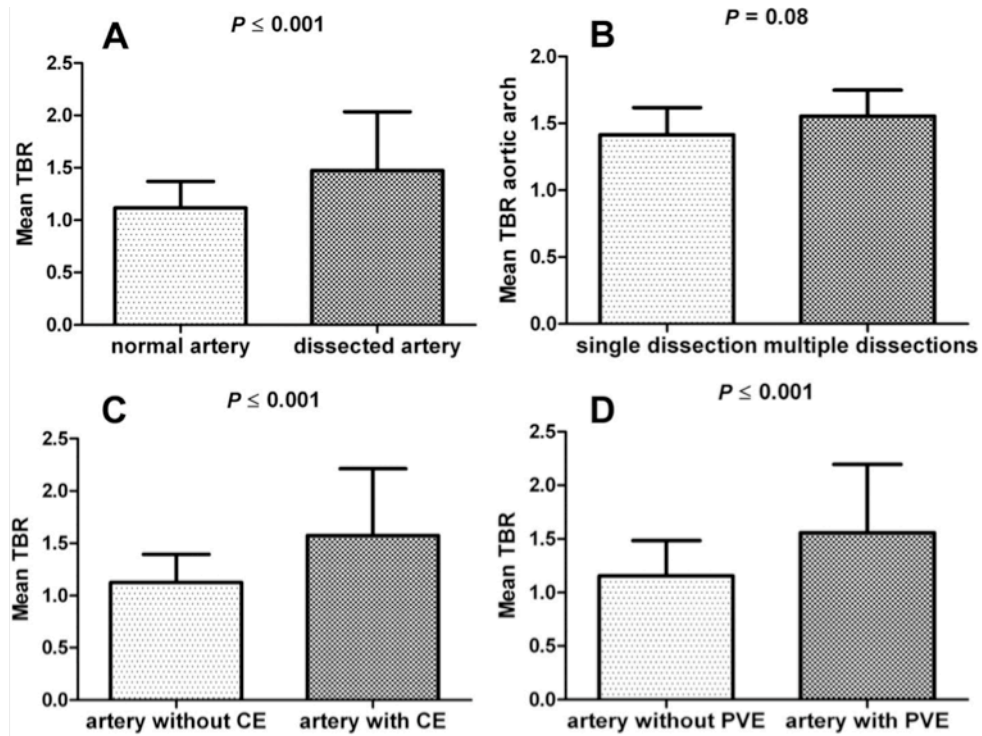


Pfefferkorn T et al. *Stroke* 2011;42:1563-1568

American Heart Association 
Learn and Live

Copyright © American Heart Association

Figure 5

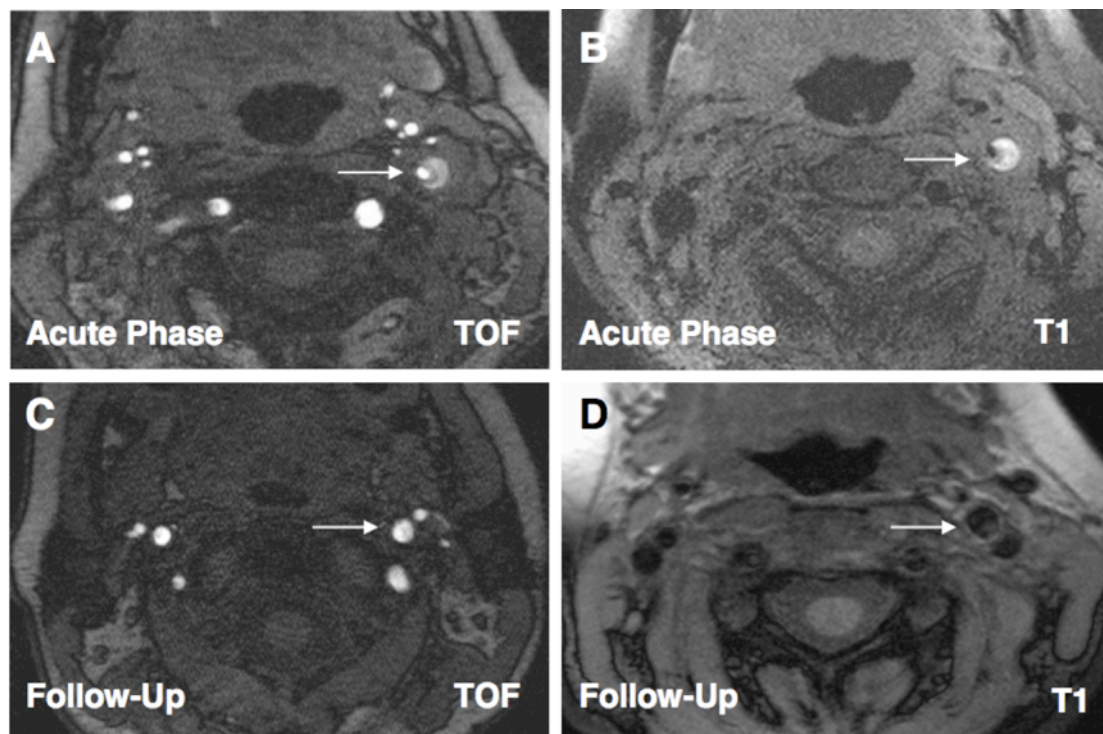


Pfefferkorn T et al. Stroke 2011;42:1563-1568



Copyright © American Heart Association

Figure S1



Pfefferkorn T et al. *Stroke* 2011;42:1563-1568

Copyright © American Heart Association

American Heart
Association 
Learn and Live

**Age determination of vessel wall hematoma in spontaneous cervical artery dissection:
A multi-sequence 3T Cardiovascular Magnetic Resonance Study**

Maximilian Habs¹, Thomas Pfefferkorn², Clemens Cyran¹, Jochen Grimm¹, Axel Rominger³, Marcus Hacker³, Christian Opherke², Maximilian Reiser¹, Konstantin Nikolaou¹, Tobias Saam¹

Author Affiliations

¹ Dept. of Clinical Radiology, University of Munich, Grosshadern Campus, Munich, Germany

² Dept. of Neurology, University of Munich, Grosshadern Campus, Munich, Germany

³ Department of Nuclear Medicine, University of Munich, Grosshadern Campus, Munich, Germany

Correspondence

PD Dr. med. Tobias Saam, MD
Institute of Clinical Radiology, Klinikum Großhadern
University of Munich
Pettenkoferstr. 8a
80336 München
Germany
Phone: +49 89 5160 9285
Fax: +49 89 5160 9282
E-mail: Tobias.Saam@med.lmu.de

Abstract

Background: Previously proposed classifications for carotid plaque and cerebral parenchymal hemorrhages are used to estimate the age of hematoma according to its signal intensities on T1w and T2w MR images. Using these classifications, we systematically investigated the value of cardiovascular magnetic resonance (CMR) in determining the age of vessel wall hematoma (VWH) in patients with spontaneous cervical artery dissection (sCAD).

Methods: 35 consecutive patients (mean age 43.6 ± 9.8 years) with sCAD received a cervical multi-sequence 3T CMR with fat-saturated black-blood T1w-, T2w- and TOF images. Age of sCAD was defined as time between onset of symptoms (stroke, TIA or Horner's syndrome) and the CMR scan. VWH were categorized into hyperacute, acute, early subacute, late subacute and chronic based on their signal intensities on T1w- and T2w images.

Results: The mean age of sCAD was 2.0, 5.8, 15.7 and 58.7 days in patients with acute, early subacute, late subacute and chronic VWH as classified by CMR ($p < 0.001$ for trend). Agreement was moderate between VWH types in our study and the previously proposed time scheme of signal evolution for cerebral hemorrhage, Cohen's kappa 0.43 ($p < 0.001$). There was a strong agreement of CMR VWH classification compared to the time scheme which was proposed for carotid intraplaque hematomas with Cohen's kappa of 0.74 ($p < 0.001$).

Conclusions: Signal intensities of VWH in sCAD vary over time and multi-sequence CMR can help to determine the age of an arterial dissection. Furthermore, findings of this study suggest that the time course of carotid hematomas differs from that of cerebral hematomas.

Keywords: CMR – internal carotid artery dissection – vertebral artery dissection – hematoma – stroke

Background

Spontaneous cervical artery dissection (sCAD) is an increasingly recognized cause of ischemic stroke, particularly in younger patients.¹ Timely diagnosis is mandatory, as instant anticoagulation or antithrombotic therapy can help to prevent more serious complications.² Clinical symptoms are often nonspecific. Therefore diagnosis may be facilitated by dedicated imaging techniques. Several studies have shown that cardiovascular magnetic resonance (CMR) is ideally suited to establish the diagnosis of sCAD by identifying the vessel wall hematoma (VWH) using fat suppressed T1-weighted images.³⁻⁵ Due to the nonspecific symptoms of the disease, diagnosis is often delayed and it is often not possible to determine the exact onset of the patients' symptoms. Thus, the exact age of the arterial dissection often remains unknown. However, this information is useful as it has been shown that half of recurrent strokes / transient ischemic attacks in sCAD patients occur within the first 2 weeks after the event⁶ and the anti-coagulation and anti-thrombotic therapies can be life threatening.

VWH is hypothesized to result from an intimal tear, allowing the blood to enter into the vessel wall, or from a rupture of the vasa vasorum. Both may lead to lumen stenosis or occlusion.⁷ It is well known, that MR signal intensities of brain hematomas and hematomas in carotid atherosclerotic plaques change over time, due to the stepwise degradation of hemoglobin.⁸⁻¹¹ Gomori et al categorized cerebral hemorrhages into hyperacute (<24 hours), acute (1-3 days), early subacute (>3 days), late subacute (>7 days) and chronic (>14 days) according to its signal intensities on T1- and T2-weighted images. In 1982, Lusby et al proposed a histological classification of carotid hematomas into fresh (< 1 week), recent (1-6 weeks) and old (> 6 weeks).¹² Chu et al¹³ showed that high-resolution CMR at 1.5T is able to identify hemorrhages in carotid atherosclerotic plaques (intraplaque hemorrhage = IPH) with good correlation to histopathology and that CMR is able to differentiate between different stages of hemorrhage according to the signal intensities on T1w and T2w images. However, a recent *in vivo* CMR study with 40 transient ischemic attack/stroke patients with ipsilateral <70% carotid stenosis showed that in 11 out of 12 patients with intraplaque hemorrhage at baseline, the hemorrhage signal remained unchanged over a 1-year period,⁴ indicating that the time course of carotid intraplaque hematomas differs from that of cerebral hematomas.

The purpose of our study was to use the above mentioned classifications for carotid plaque and cerebral parenchymal hemorrhages to systematically investigate the value of CMR in determining the age of vessel wall hematoma (VWH) in patients with spontaneous cervical artery dissection.

Methods

Patient Selection

A total of 35 patients were enrolled in this prospective, monocentric observational study, which had been approved by the local institutional ethics committee. Patients with a first manifestation of spontaneous cervical artery dissection were included in the study if the following inclusion criteria were fulfilled: 1) no contraindication for CMR and unequivocal CMR evidence (intramural hematoma) of cervical artery dissection and 2) written informed consent. The date of dissection was estimated from the first appearance of one or more of the following symptoms or signs: Horner's syndrome, transient ischemic attack or stroke. If patients had > than one dissection only the artery was used for further analysis which contributed to the patients' symptoms (index artery). Patients with nonspecific symptoms (e.g. neck pain), a history of a related trauma, a pre-existing diagnosis of arteritis / vasculitis (e. g. Takayasu arteritis) or an underlying disease clearly associated with cervical artery dissection (e. g. Marfan syndrome) were excluded.

MR Imaging Protocol

We used a multi-sequence CMR protocol 15 without ECG gating or motion correction to image the cervical arteries with a 3.0 Tesla MR scanner (Magnetom Verio, Siemens Healthcare, Erlangen, Germany) using a 12-channel head coil and a dedicated four-channel surface coil (Machnet, Eelde, Netherlands). Each patient was scanned once with the same protocol which included a fat- and blood suppressed 2D-T1 Turbo Spin Echo (TSE) sequence [TR=800 ms, TE=12 ms], a fat- and blood suppressed 2D-T2 TSE sequence [TR=3000 ms, TE=65 ms] and a 3D-GRE time-of-flight angiography (TOF) [TR=21 ms, TE=3.96 ms]. Coverage was from the carotid bifurcation to the origin of the basilar artery. Best in plane resolution was 0.5 x 0.5 mm² with a slice thickness of 4 mm for T1- and T2- weighted images and 1 mm for TOF images with a field of view of 160*120 mm². Number of slices was 20 – 30 for T1-, 24-36 for T2- and 104 for TOF images. Parallel-imaging with a PAT factor of 2 was used for all sequences using the generalized autocalibrating partially parallel acquisition algorithm (GRAPPA), resulting in a total scan time of 15-20 minutes, depending on the number of slices.^{15,16} Figure 1 shows the applied sequences.

Image Analysis

Two radiologists with more than 5 years experience in black blood carotid artery imaging (T.S., K.N.) reviewed all cases and determined the affected vessels, the location of the VWH and its signal intensities. Both reviewers were blinded to clinical data. In case of any discrepant findings between the two readers, a final diagnosis was made in consensus. The age of hemorrhage within VWH was categorized on a 5-point scale into hyperacute, acute, early subacute, late subacute and chronic, based on the relative signal intensities of the hematoma on the T1w- and T2w- images compared to the normal vessel wall (in analogy to cerebral hemorrhage, [Table 1](#)). If vessel wall hematomas had mixed signal intensities, the hematoma was classified according to the oldest hemorrhage type present within the hematoma. If patients had more than one dissection, only the artery that contributed to the patient's symptoms was used for further analysis. [Figure 2](#) shows examples for the different presentations of VWH signal intensities.

Since a VWH can extend over several segments of an artery, its location was determined by the most proximal appearance. For the internal carotid artery (ICA) the beginning of the VWH was classified as either cervical / extracranial (C1 segment) or intracranial (C2 to C7 segment).¹⁷ The beginning of the VWH in the vertebral artery (VA) was described using the typical division of the VA into 4 segments (V1, V2, V3, V4) with V1 being the most proximal and V4 the intracranial part of the artery. The level of stenosis was evaluated according to the North American Symptomatic Carotid Endarterectomy Trial (NASCET) criteria on TOF images, i.e. comparing the measured lumen diameter at the site of dissection with the diameter at a more distal location with a normal lumen diameter.

Classification Schemes of Cerebral and Carotid Hematomas

Gomori et al categorized cerebral hemorrhages into hyperacute (<24 hours), acute (1-3 days), early subacute (>3 days), late subacute (>7 days) and chronic (>14 days)¹¹ according to its signal intensities on T1- and T2-weighted images (see [Table 1](#)). In 1982, Lusby et al proposed a histological classification of carotid hematomas into fresh (< 1 week), recent (1-6 weeks) and old (> 6 weeks) based on the cellular features seen by elastochrome staining. Here fresh hemorrhage showed intact red blood cells, polymorph nuclear infiltrates and focal macrophage activity. Recent hemorrhage was characterized by hemorrhagic debris and macrophage engulfment of hemosiderin. Old hemorrhage was characterized by amorphous material surrounded by fibrous tissue.¹²

Statistical Analysis

Statistical analysis was carried out with SPSS version 16.0. We compared quantitative variables of groups using independent t-test. Differences of distribution regarding nominal variables in groups were analyzed with Fisher's exact test. The level of agreement between hemorrhage classifications was measured using Cohen's kappa coefficient with values < 0 indicating no agreement and 0–0.20 as slight, 0.21–0.40 as fair, 0.41–0.60 as moderate, 0.61–0.80 as strong and 0.81–1.00 as almost perfect agreement. A p-value ≤ 0.05 (two-sided) was considered significant. Figures were generated using the software GraphPad Prism version 5.

Results

Patient Characteristics

43 patients with cervical artery dissection fulfilled the inclusion criteria. 8 patients were excluded due to traumatic dissection (n=3), vasculitis (n=2), nonspecific symptoms (n=2), and fibromuscular dysplasia (n=1). [Table 2](#) gives an overview of the demographics, clinical presentation and cardiovascular risk factors. The mean age of all patients was 43.6 years, range 30–61 years. The mean interval between the onset of symptoms and the CMR scan was 22 ± 25 days. 26 out of 35 patients (74.3%) of our patients presented with a sensomotoric deficit as initial symptom and 9 patients (26.7%) had an isolated Horner's syndrome. 6 out of 35 patients (17.2%) had a Horner's syndrome *and* a sensomotoric deficit due to the sCAD. Of the 26 patients with a sensomotoric deficit, 16 were diagnosed with a stroke and 10 with a transient ischemic attack (TIA).

CMR Data:

Vessels Affected and Degree of Stenosis

In 35 patients we observed a total of 47 sCAD. 18 patients (51%) presented with single ICA dissections, 7 patients (20%) presented with single VA dissections and 10 patients (29%) suffered from multiple artery dissections. Only the 35 index arteries which contributed to the patients' symptoms were used for further analysis. 24 index arteries were in the ICA and 11 in the VA. We detected 7 total occlusions through VWH or thrombus within 35 dissections (20%) and measured a mean level of stenosis in the non-occluded arteries of 61%. Although the percentage of stroke

in single VA dissections tended to be higher than in single ICA dissections (71% vs. 40%), those findings were not statistically significant. Overall the occurrence of stroke was not associated with a significant higher level of stenosis (65% vs. 55%; $p=0.5$). Patients with total occlusions of the affected artery tended to have a higher incidence of stroke (71% vs. 40%; $p=0.13$).

VWH in ICA dissections was significantly more often seen in the intracranial portion (C2-C7 segments) than in the cervical portion (C1 segment) of the artery (80% vs. 20%; $p<0.05$). The most common location of the VWH in VA dissections was the V2 segment (55%) and the V3 segment (36%). Only one VA dissection started in the V1 segment and no dissection originated from the V4 segment.

Age of Vessel Wall Hematoma in CMR

We observed no case of hyperacute hemorrhage. One patient who suffered a sCAD two days before, the CMR scan displayed imaging characteristics of an acute VWH. Six patients showed MR characteristics of early subacute hemorrhage with a mean imaging interval of 5.8 days, range 1-13 days. In 21 patients VWH was classified as late subacute hemorrhage according to CMR, with a mean imaging interval of 15.7 days, range 4-37 days. Seven patients showed MR characteristics of chronic VWH with a mean age of the dissection of 58.7 days, range 33-125 days. Mean age of sCAD was 2.0, 5.8, 15.7 and 58.7 days in patients with acute, early subacute, late subacute and chronic VWH ($p<0.001$ for trend). There was only a moderate agreement between the chronological development of the MR signal changes seen in cerebral hemorrhage and the evolution of VWH in CMR with a Cohen's kappa of 0.43 ($p<0.001$, see [Table 3](#)). However, when we compared our classification with the classification of carotid intraplaque hemorrhages which was proposed by Lusby et al in 1982,¹² there was strong agreement with a Cohen's kappa of 0.74 ($p<0.001$, see [Table 4](#)). [Figure 3](#) illustrates the presentation and typical signal characteristics of the different VWH types. 6 of the 35 index arteries (17%) had a VWH with mixed signal intensities and were classified according to the oldest component of hematoma ([Figure 4](#)).

Discussion

Our study showed that MR signal intensities of VWH are dependent on the age of the sCAD. More specifically, the age of the VWHs which were classified into acute, early subacute, late subacute and chronic hematomas according to its signal intensities on the T1w and T2w images differed, suggesting that *in vivo* CMR might be useful in determining the age of a sCAD. Given the fact that the risk of recurrent TIA or stroke is highest in the first two weeks after a sCAD⁶ this information could be useful in patients with nonspecific initial symptoms, in whom the age of the sCAD is not known. From a clinical perspective, patients with more acute hematomas may therefore require a closer clinical observation than those with chronic hematomas. Furthermore, this information could be useful in cases where it is not clear whether the arterial dissection is spontaneous or traumatic. E.g., a patient with an arterial dissection and signs of an early subacute hemorrhage as determined by CMR, who suffered a car accident four weeks ago, will most likely have had a spontaneous dissection rather than a traumatic one.

Finally, this multi-sequence MR protocol could give us new insights into the pathogenesis of the disease, especially in patients with multiple dissections, where the age of the VWH may be different for each individual affected vessel.¹⁸ The MR signal changes observed in our study had only moderate agreement with the dynamics seen in cerebral hematomas (Cohen's kappa of 0.43; $p < 0.001$), suggesting that the time course of signal intensity changes varies in different body regions and organs. In contrast we found strong agreement with a previously proposed histology classification of carotid plaque hematomas¹² with a Cohen's kappa value of 0.74 ($p < 0.001$). However, in the study of carotid endarterectomy specimen of Lusby et al it is not clear how the age of the hematomas was determined and there is increasing evidence that MR signal characteristics of carotid intraplaque hematomas in atherosclerotic disease remain stable over a one year time period in most cases as has been suggested by Takaya et al¹⁹ and Kwee et al¹⁴. These differences in the speed of hematoma decomposition might be explained by recurrent microbleeds into the atherosclerotic hematomas, which are caused by leaky neovessels.²⁰ In the present study, 83% of the investigated VWH had a homogeneous appearance that could easily be staged due to their signal characteristics. The homogeneous appearance of the VWH supports the theory of a one-time event of sCAD in most cases. Only 17% of the VWH had mixed signal intensities, which could either indicate recurrent hemorrhages or a different speed of decomposition. All of these cases had a mix of acute, early and late subacute hematomas, which were then classified as late subacute hematomas (Figure 4).

Similar to previous studies, different segments of the VA and ICA have different propensities to develop a VWH.²¹⁻²⁴ More specifically, ICA dissections tend to occur significantly more often in the intracranial segment than in the cervical segment of the carotid artery (80% vs. 20%; $p < 0.05$). The most common location for VA dissections was the V2 (55%) and the V3 (36%) segment. Only one VA dissection started in the V1 segment and no dissection originated from the V4 segment. This is similar to findings of a study of 169 patients with VA dissection²² who found incidences of 20%, 34%, 35% and 11% for the V1, V2, V3 and V4 segment, respectively.

About half the patients in our study (46%) developed a stroke. No significant relation was observed between the level of stenosis in dissected vessels and the occurrence of stroke (70% vs. 65%; $p=0.7$). This supports the theory of Benninger et al²⁵ that a thromboembolic stroke-mechanism is probably more likely than hemodynamic effects in cervical artery dissection patients.

Limitations

Although a CMR classification of VWH in sCAD patients seems feasible, our study has several limitations: since diagnostic workup for a patient with a fresh manifestation of cervical artery dissection takes time, we were not able to evaluate the hyperacute stage of hemorrhage and only one patient with the signal characteristics of acute hemorrhage was acquired. In general a longitudinal, rather than a cross-sectional study design would be more conclusive. Repeated scans of individual patients with cervical artery dissection within short intervals of time are necessary for a better understanding of the time course of the signals changes. Furthermore it can be difficult to determine the exact time between the occurrence of sCAD and the CMR scan. Therefore we included only patients with symptoms, such as TIA, stroke or Horner's syndrome, which could be clearly attributed to the sCAD. However, we cannot exclude that some patients might initially have had an asymptomatic sCAD and a recurrent episode of VWH a couple of days later causing the symptoms. However, the majority of our patients had homogeneous VWHs which could be clearly categorized into acute, early subacute, late subacute or chronic. Only 17% of all VWHs had mixed signal intensities, suggesting that either the speed of decomposition differed at different segments of the arteries or that these patients had a recurrence of VWH.

Conclusions

Magnetic resonance imaging signal intensities of VWH in sCAD vary over time and multi-sequence CMR can help to determine the age of an arterial dissection. Furthermore, findings of this study suggest that the signal intensity change of carotid hematomas differs from that of cerebral hematomas, suggesting a different time course of decomposition. VWH classification by CMR in patients with sCAD could be useful to improve our understanding of the pathophysiology of the disease, by helping to identify potential causes of the disease, e.g. traumatic versus spontaneous dissections. It could also help to improve risk stratification of recurrent TIA / stroke especially in patients with nonspecific initial symptoms, where the age of the sCAD is not exactly known.

Competing interests

The authors declare that they have no competing interests.

Author's contributions

MH, TP, CCC, JG, AR, MAH, CO, KN, MFR and TS were involved in the study concept/study. MH, TP and TS were involved in data analysis/interpretation. MH, TP, CCC, JG, AR, MAH, CO, KN, MFR and TS were involved in manuscript preparation and editing. MH, TP, CCC, JG, AR, MAH, CO, KN, MFR and TS gave final approval of the submitted manuscript.

References

1. Debette S, Leys D. Cervical-artery dissections: Predisposing factors, diagnosis, and outcome. **Lancet Neurol.** 2009;8:668-678
2. Georgiadis D, Arnold M, von Buedingen HC, Valko P, Sarikaya H, Rousson V, Mattle HP, Boussier MG, Baumgartner RW. Aspirin vs anticoagulation in carotid artery dissection: A study of 298 patients. **Neurology.** 2009;72:1810-1815
3. Oppenheim C, Naggara O, Touze E, Lacour JC, Schmitt E, Bonneville F, Crozier S, Guegan-Massardier E, Gerardin E, Leclerc X, Neau JP, Sirol M, Toussaint JF, Mas JL, Meder JF. High-resolution MR imaging of the cervical arterial wall: What the radiologist needs to know. **Radiographics.** 2009;29:1413-1431
4. Naggara O, Touze E, Marsico R, Leclerc X, Nguyen T, Mas JL, Pruvo JP, Meder JF, Oppenheim C. High-resolution MR imaging of periarterial edema associated with biological inflammation in spontaneous carotid dissection. **Eur Radiol.** 2009;19:2255-2260
5. Bachmann R, Nassenstein I, Kooijman H, Dittrich R, Kugel H, Niederstadt T, Kühlenbaumer G, Ringelstein EB, Kramer S, Heindel W. Spontaneous acute dissection of the internal carotid artery: High-resolution magnetic resonance imaging at 3.0 tesla with a dedicated surface coil. **Invest Radiol.** 2006;41:105-111
6. Schwartz NE, Vertinsky AT, Hirsch KG, Albers GW. Clinical and radiographic natural history of cervical artery dissections. **J Stroke Cerebrovasc Dis.** 2009;18:416-423
7. Schievink WI. Spontaneous dissection of the carotid and vertebral arteries. **N Engl J Med.** 2001;344:898-906
8. Gomori JM, Grossman RI. Mechanisms responsible for the mr appearance and

evolution of intracranial hemorrhage. **Radiographics**. 1988;8:427-440

9. Gomori JM, Grossman RI, Hackney DB, Goldberg HI, Zimmerman RA, Bilaniuk LT. Variable appearances of subacute intracranial hematomas on high-field spin-echo MR. **AJR Am J Roentgenol**. 1988;150:171-178
10. Gomori JM, Grossman RI, Steiner I. High-field magnetic resonance imaging of intracranial hematomas. **Isr J Med Sci**. 1988;24:218-223
11. Gomori JM, Grossman RI, Yu-IP C, Asakura T. NMR relaxation times of blood: Dependence on field strength, oxidation state, and cell integrity. **J Comput Assist Tomogr**. 1987;11:684-690
12. Lusby RJ, Ferrell LD, Ehrenfeld WK, Stoney RJ, Wylie EJ. Carotid plaque hemorrhage. Its role in production of cerebral ischemia. **Arch Surg**. 1982;117:1479-1488
13. Chu B, Kampschulte A, Ferguson MS, Kerwin WS, Yarnykh VL, O'Brien KD, Polissar NL, Hatsukami TS, Yuan C. Hemorrhage in the atherosclerotic carotid plaque: A high-resolution MRI study. **Stroke**. 2004;35:1079-1084
14. Kwee RM, van Oostenbrugge RJ, Mess WH, Prins MH, van der Geest RJ, Ter Berg JW, Franke CL, Korten AG, Meems BJ, van Engelshoven JM, Wildberger JE, Kooi ME. Carotid plaques in transient ischemic attack and stroke patients: One-year follow-up study by magnetic resonance imaging. **Invest Radiol**. 2010;45(12):803-9.
15. Saam T, Raya JG, Cyran CC, Bochmann K, Meimarakis G, Dietrich O, Clevert DA, Frey U, Yuan C, Hatsukami TS, Werf A, Reiser MF, Nikolaou K. High resolution carotid black-blood 3T MR with parallel imaging and dedicated 4-channel surface coils. **J Cardiovasc Magn Reson**. 2009;11:41
16. Saam T, Habs M, Cyran CC, Grimm J, Pfefferkorn T, Schuller U, Reiser MF,

Nikolaou K. New aspects of MRI for diagnostics of large vessel vasculitis and primary angiitis of the central nervous system. *Radiologe*. 2010;50(10):861-71.

17. Osborn AG, Salzman KL, Barkovich AJ. **Diagnostic imaging**. Brain. Salt Lake City, Utah: Amirsys; 2010.
18. Dittrich R, Nassenstein I, Bachmann R, Maintz D, Nabavi DG, Heindel W, Kühlenbaumer G, Ringelstein EB. Polyarterial clustered recurrence of cervical artery dissection seems to be the rule. **Neurology**. 2007;69:180-186
19. Takaya N, Yuan C, Chu B, Saam T, Polissar NL, Jarvik GP, Isaac C, McDonough J, Natiello C, Small R, Ferguson MS, Hatsukami TS. Presence of intraplaque hemorrhage stimulates progression of carotid atherosclerotic plaques: A high-resolution magnetic resonance imaging study. **Circulation**. 2005;111:2768-2775
20. Virmani R, Kolodgie FD, Burke AP, Finn AV, Gold HK, Tulenko TN, Wrenn SP, Narula J. Atherosclerotic plaque progression and vulnerability to rupture: Angiogenesis as a source of intraplaque hemorrhage. **Arterioscler Thromb Vasc Biol**. 2005;25:2054-2061
21. Arnold M, Kurmann R, Galimanis A, Sarikaya H, Stapf C, Gralla J, Georgiadis D, Fischer U, Mattle HP, Boussier MG, Baumgartner RW. Differences in demographic characteristics and risk factors in patients with spontaneous vertebral artery dissections with and without ischemic events. **Stroke**. 2010;41:802-804
22. Arnold M, Boussier MG, Fahrni G, Fischer U, Georgiadis D, Gandjour J, Benninger D, Sturzenegger M, Mattle HP, Baumgartner RW. Vertebral artery dissection: Presenting findings and predictors of outcome. **Stroke**. 2006;37:2499-2503
23. Mokri B, Houser OW, Sandok BA, Piepgras DG. Spontaneous dissections of the vertebral arteries. **Neurology**. 1988;38:880-885

24. Kirsch E, Kaim A, Engelter S, Lyrer P, Stock KW, Bongartz G, Radu EW. MR-angiography in internal carotid artery dissection: Improvement of diagnosis by selective demonstration of the intramural haematoma. **Neuroradiology**. 1998;40:704-709
25. Benninger DH, Georgiadis D, Kremer C, Studer A, Nedeltchev K, Baumgartner RW. Mechanism of ischemic infarct in spontaneous carotid dissection. **Stroke**. 2004;35:482-485

Table 1**Relative signal intensities for different types of cerebral hemorrhage (adapted from Gomori et al [11])**

Type of Hemorrhage	T1 w	T2 w	Histology
Hyperacute	-	↑	Intracellular oxyhemoglobin
Acute	↓ or -	↓	Intracellular deoxyhemoglobin
Early subacute	↑	↓	Intracellular methemoglobin
Late subacute	↑	↑	Extracellular methemoglobin
Chronic	↓	↓	Hemosiderin

All signal intensities relative to the normal carotid wall

↓ hypointense

↑ hyperintense

- isointense

Habs et al. *Journal of Cardiovascular Magnetic Resonance* 2011 **13**:76 doi:10.1186/1532-429X-13-76

[OPEN](#) [DATA](#)

Table 2: Patient characteristics

	Study population (n=35)
	Mean \pm SD (range) or %
Age, y	43.6 \pm 9.8 (30-61)
Male sex, %	60.0 (21/35)
BMI, kg/m ²	24.2 \pm 4.2 (19.7-41.7)
MR Imaging	
Age of the dissection	22.3 \pm 24.9 (1-125)
Total occlusion, %	20.0 (7/35)
Stenosis, %	61.4 \pm 33.9 (0-100)
<i>Internal Carotid Artery Dissection</i>	69 (24/35)
Extracranial C1 Segment, %	20 (5/24)
Intracranial C1 Segment, %	80 (19/24)
<i>Vertebral Artery Dissection</i>	31 (11/35)
V1 Segment, %	9 (1/11)
V2 Segment, %	55 (6/11)
V3 Segment, %	36 (4/11)
V4 Segment, %	0 (0/11)
<i>Type of Vessel Wall Hematoma</i>	
Acute, %	3 (1/35)
Early Subacute, %	17 (6/35)
Late Subacute, %	60 (21/35)
Chronic, %	20 (7/35)
Symptoms	
Stroke, %	45.7 (16/35)
Transient Ischemic Attack, %	28.6 (10/35)
Horner's Syndrome, %	42.9 (15/35)
Cardiovascular Risk Factors	
Current smoker, %	34.3 (12/35)
Former smoker, %	25.7 (9/35)
Hypertension, %	31.4 (11/35)
Hypercholesterolemia, %	25.7 (9/35)
Diabetes, %	0.0 (0/35)
Family history of cardiovascular events, %	17.1 (6/35)

Table 3**VWH age classified after criteria proposed by Gomori et al**

	<1 Day	1-3 Days	4-7 Days	8-14 Days	>14 Days
Observations (n = 35)	0	n = 2	n = 6	n = 10	n = 17
Hyperacute (n = 0)	0	0	0	0	0
Acute (n = 1)	0	1	0	0	0
Early subacute (n = 6)	0	1	4	1	0
Late subacute (n = 21)	0	0	2	9	10
Chronic (n = 7)	0	0	0	0	7

Habs et al. Journal of Cardiovascular Magnetic Resonance 2011 **13**:76 doi:10.1186/1532-429X-13-76[OPEN DATA](#)

Table 4**VWH age classified after criteria proposed by Lusby et al**

	<1 Week	1-6 Weeks	>6 Weeks
Observations (n = 35)	n = 8	n = 22	n = 5
Fresh hemorrhage (n = 7)	6	1	0
Recent hemorrhage (n = 21)	2	19	0
Old hemorrhage (n = 7)	0	2	5

Habs et al. *Journal of Cardiovascular Magnetic Resonance* 2011 **13**:76 doi:10.1186/1532-429X-13-76

[OPEN DATA](#)

Figure legends

Figure 1: Multi sequence CMR (TOF angiography, T1w- and T2w- images) of a 47-year old patient with spontaneous cervical artery dissection of the left ICA. The patient presented with a left sided Horner's Syndrome. The VWH (arrows), bright in TOF and T1w images, originated from the proximal C1 segment of the ICA.

Figure 2: Types of hemorrhage as determined by multi sequence CMR in different patients. Line 1 shows an acute VWH of the left ICA, 2 days after onset of symptoms. Line 2 shows an early subacute VWH of the right VA with an imaging interval of 12 days. Line 3 shows a late subacute VWH of the right ICA after 17 days. Line 4 shows a chronic VWH of the left VA after 50 days.

Figure 3: Distribution of time intervals and type of hemorrhage as determined by CMR. Dotted line indicates Mean. Whiskers indicate standard deviation of the Mean. Squares represent each patient.

Figure 4: Multi sequence CMR showing VWH (chevron) of the right VA in the V2 segment with mixed signal intensities in a 34-year-old patient with sCAD. The hematoma presents with imaging features of acute, early subacute and late subacute hemorrhage. The VWH was classified according to the oldest hemorrhage type present (i.e. late subacute). CMR interval from onset of symptoms to scan was 9 days.

Figure 1

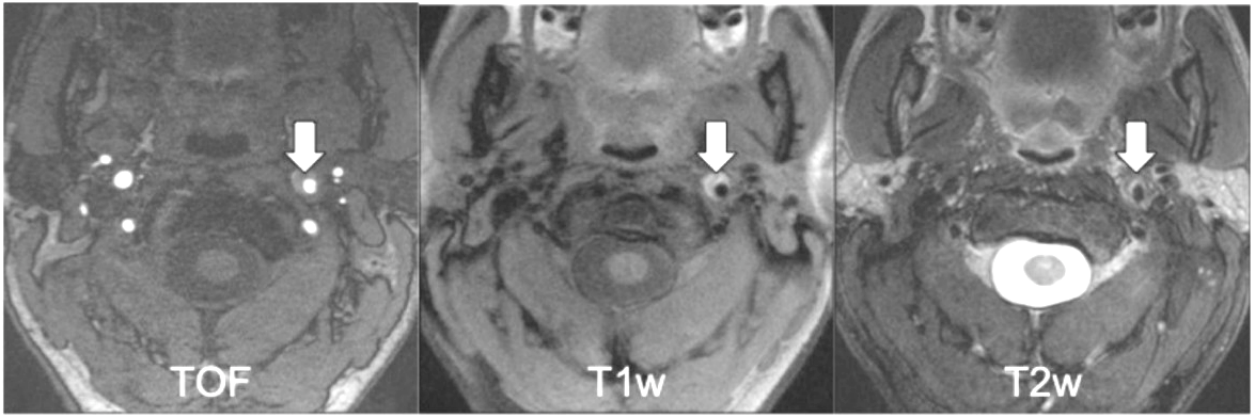


Figure 2

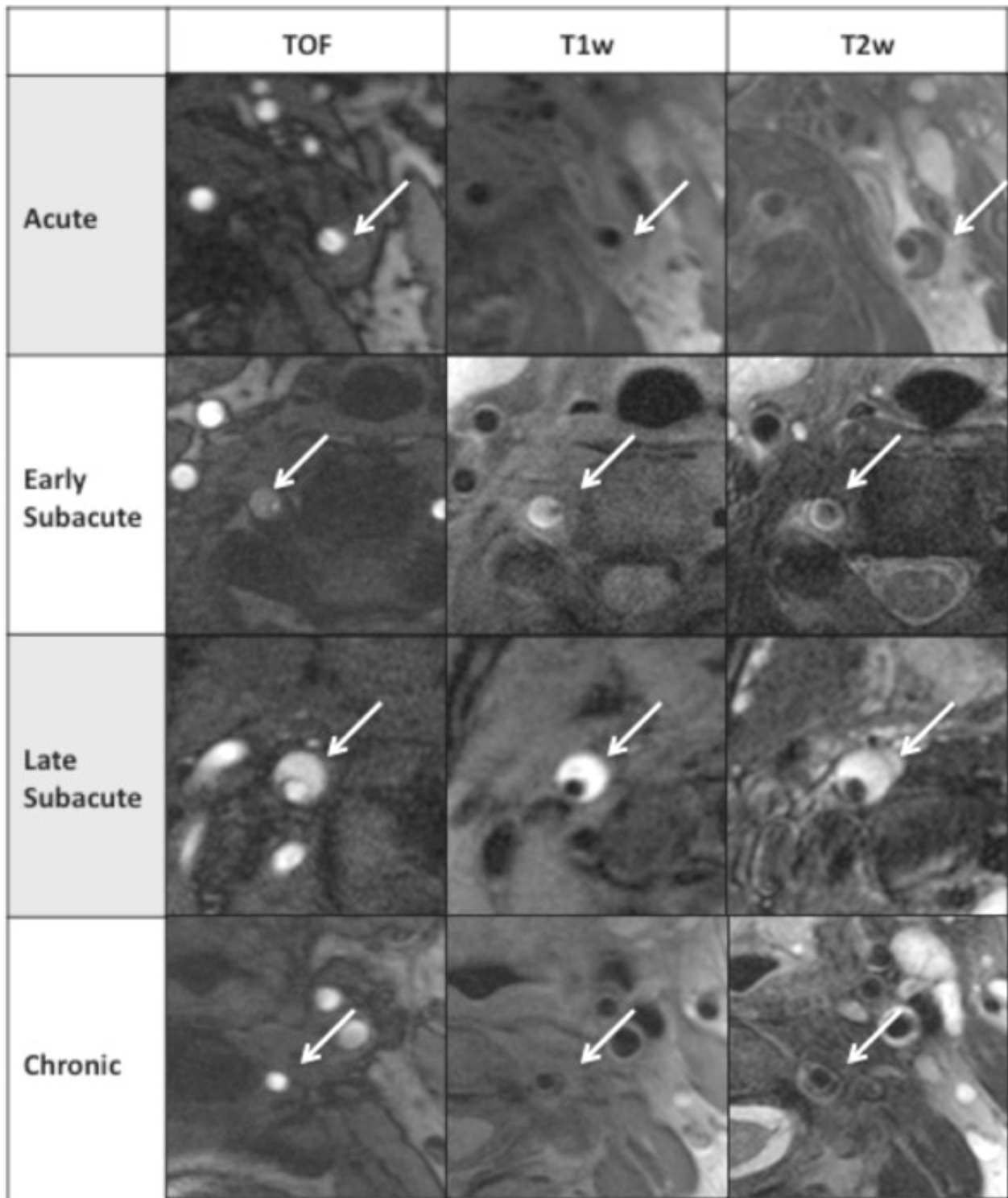


Figure 3

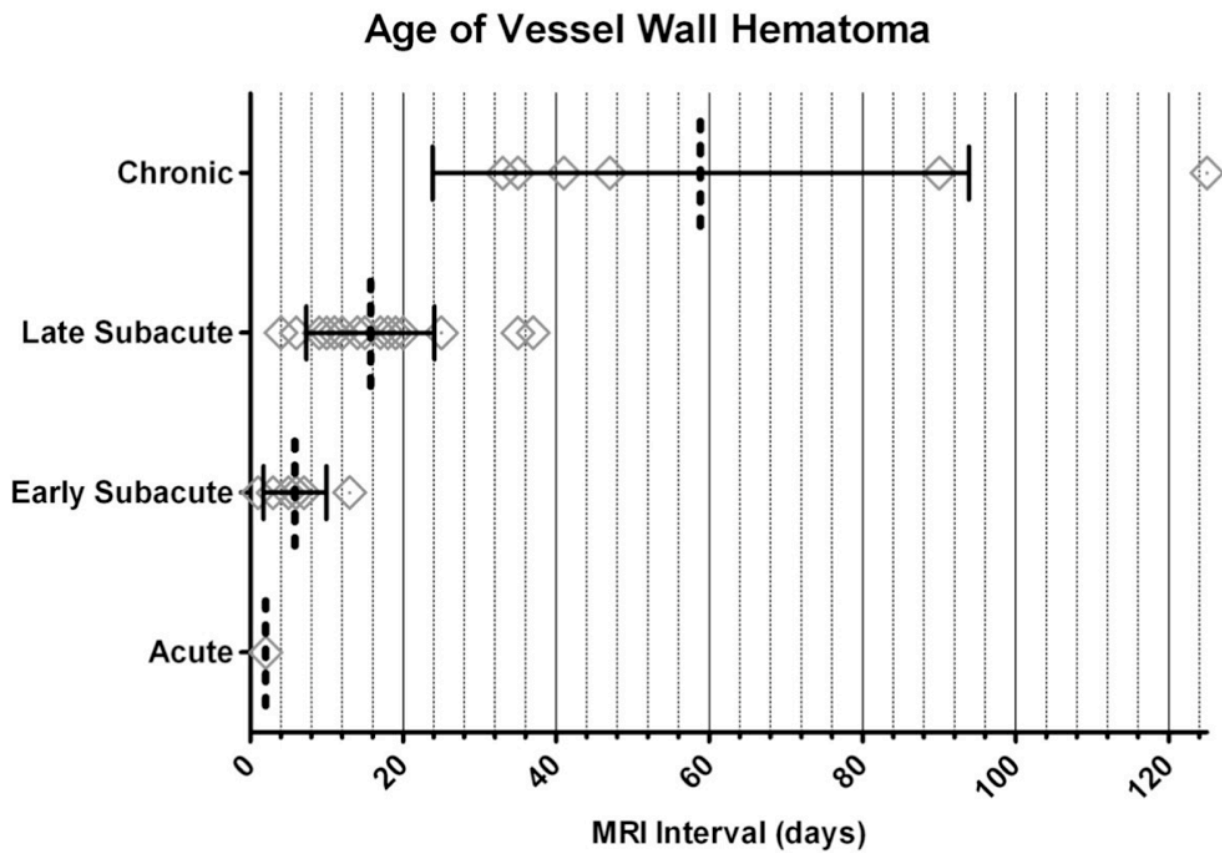
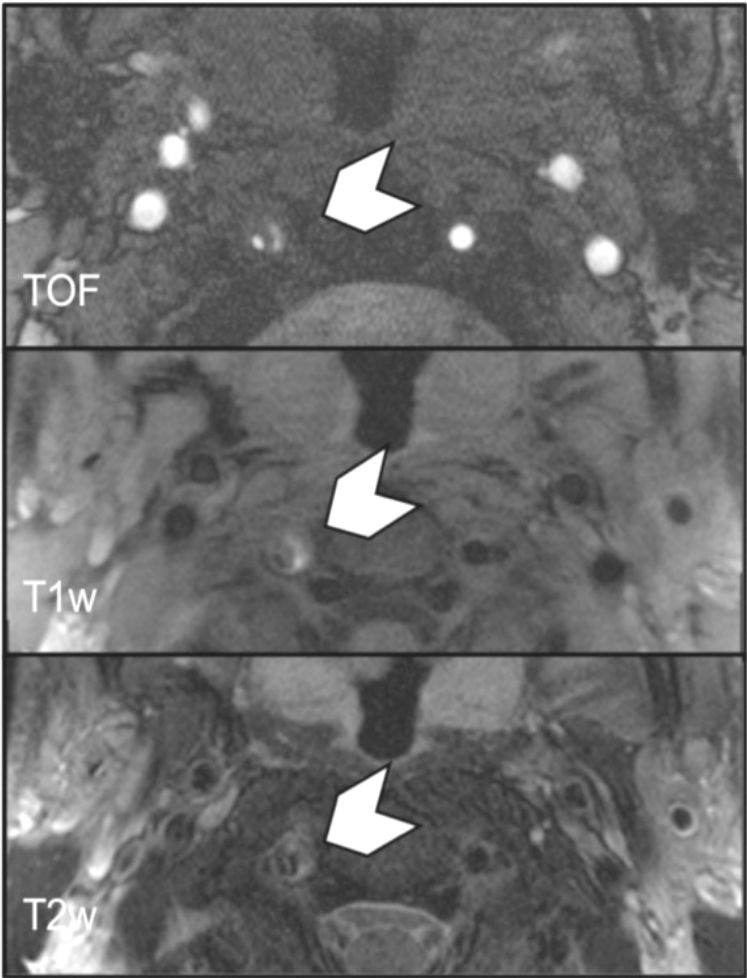


Figure 4



3. VERÖFFENTLICHUNGEN

Original Arbeiten

Pfefferkorn T, Saam T, Rominger A, Habs M, Gerdes L, Schmidt C, Cyran C, Straube A, Linn J, Nikolaou K, Bartenstein P, Reiser M, Hacker M, Dichgans M. Vessel wall inflammation in spontaneous cervical artery dissection: a prospective, observational positron emission tomography, computed tomography, and magnetic resonance imaging study **Stroke**. 2011 Jun;42(6):1563-8. Epub 2011 Apr 21. Impact Factor 5.756

Cyran CC, Sourbron S, Bochmann K, Habs M, Pfefferkorn T, Rominger A, Raya JG, Reiser MF, Dichgans M, Nikolaou K, Hacker M, Saam T. Quantification of supra-aortic arterial wall inflammation in patients with arteritis using high resolution dynamic contrast-enhanced magnetic resonance imaging: initial results in correlation to [18F]-FDG PET/CT. **Invest Radiol**. 2011 Sep;46(9):594-9. Impact Factor 4.670

Habs M, Pfefferkorn T, Cyran CC, Grimm J, Rominger A, Hacker M, Opherk C, Reiser MF, Nikolaou K, Saam T. Age determination of vessel wall hematoma in spontaneous cervical artery dissection: A multi-sequence 3T Cardiovascular Magnetic Resonance Study. **J Cardiovasc Magn Reson**. 2011 Nov 28;13(1):76. Impact Factor: 4.330

Pfefferkorn T, Linn J, Habs M, Opherk C, Cyran C, Ottomeyer C, Straube A, MD, Dichgans M, Nikolaou K, Saam T. Black Blood MRI in suspected large artery primary angiitis of the central nervous system. **J Neuroimaging**. 2012 Feb. Accepted. Impact Factor: 1.287

Buchkapitel

Habs M, Saam T. Geriatric Imaging: Atherosclerotic Heart Disease. Publisher: Springer Science and Business Media. Veröffentlichungstermin: Sept. 2012

Review Artikel

Saam T, Habs M, Pfefferkorn T, Schueller U, Reiser MF, Nikolaou K. New aspects of MR Imaging in the diagnosis of large vessel vasculitis and primary angitis of the central nervous system. **Radiologe**. 2010 Oct;50(10):861-71. Impact Factor 0.531

Case Reports

Saam T, Habs M, Pollatos O, Cyran CC, Pfefferkorn T, Dichgans M, Dietrich O, Glaser C, Reiser MF, Nikolaou K. High-resolution black-blood contrast-enhanced T1-weighted images for the diagnosis and follow-up of intracranial arteritis. **Br J Radiol.** 2010 Sep;83(993):e182-4. Impact Factor 2.366

Vorträge und Poster

Saam T, Habs M, Rominger A, Walter L, Rist C, Schwarz F, Nikolaou K, Reiser MF, Bartenstein P, Hacker M. Impact of Cardiovascular Risk Factors and Vessel Wall Inflammation on Atherosclerotic Disease Progression: A PET/CT Study. **97th Scientific Assembly and Annual Meeting of the Radiological Society of North America, Chicago, USA**, November 27th – December 2nd, 2011, LL-NMS-WE

Saam T, Habs M, Pfefferkorn T, Hacker M, Rominger A, Cyran C, Dichgans M, Reiser MF, Nikolaou K. Bestimmung des Alters von Wandhämatomen bei Patienten mit spontanen Dissektionen der Halsgefäße mittels in vivo MRT. **92. Deutscher Röntgenkongress**, June 1st-4th 2011, Hamburg, Germany, RoFo Sonderheft 1, Mai 2011, Band 183, S225

Saam T, Pfefferkorn T, Habs M, Hacker M, Rominger A, Nikolaou K, Cyran C, Reiser MF, Dichgans M. Vessel Wall Inflammation in Spontaneous Cervical Artery Dissection: A Prospective Observational PET-CT and MRI Study. **96th Scientific Assembly and Annual Meeting of the Radiological Society of North America**, Chicago, USA, November 29th – December 4th, 2010, SST02-08

Saam T, Cyran C, Habs M, Pfefferkorn T, Dichgans M, Dietrich O, Reiser MF, Nikolaou K. Hochaufgelöste Black-Blood 3T MRT in der Diagnostik der Primären Vaskulitis des Zentralen Nervensystems. **Deutscher Röntgenkongress 2010**, May 12th-15th, Berlin, Germany, RöFo; S 1, 2010, Volume 182, VO_201.6 (Neuro I – Nicht-Ischämische Erkrankungen I)

Saam T, Pfefferkorn T, Habs M, Hacker M, Rominger A, Cyran C, Dichgans M, Reiser MF, Nikolaou K. Age of vessel wall hematoma in cervical artery dissection as determined by multi-sequence MRI. **European Congress of Radiology 2010**, March 4th-8th, Vienna, Austria. ECR 2010 Vol 1, S1,B-436

Saam T, Pfefferkorn T, Habs M, Hacker M, Rominger A, Cyran C, Dichgans M, Reiser MF, Nikolaou K. Spontaneous cervical artery dissection: an inflammatory disease? Results of a prospective observational PET-CT and MRI study. **European Congress of Radiology 2010**, March 4th-8th, Vienna, Austria. ECR 2010 Vol 1, S1,B-658

Habs M, Pfefferkorn T, Habs M, Hacker M, Rominger A, Cyran C, Dichgans M, Reiser MF, Nikolaou K, Saam T. Spontane arterielle Dissektionen der Halsgefäße: eine entzündliche Erkrankung? Ergebnisse einer prospektiven MRT- und PET/CT-Untersuchung. **Deutscher Röntgenkongress 2010**, May 12th-15th, Berlin, Germany, RöFo; S 1, 2010, Volume 182, VO_210.3 (Gefäße II – Methodenvergleich II)

Saam T, Pfefferkorn T, Habs M, Hacker M, Rominger A, Cyran C, Dichgans M, Reiser MF, Nikolaou K. Spontaneous cervical artery dissection: an inflammatory disease? Results of a prospective observational PET-CT and MRI study. **ISMRM 2010**, Stockholm, Sweden. Poster

Saam T, Habs M, Pollatos O, Cyran CC, Pfefferkorn T, Dichgans M, Dietrich O, Glaser C, Reiser MF, Nikolaou K. High-resolution black-blood contrast-enhanced T1-weighted images for the diagnosis and follow-up of intracranial arteritis. **ISMRM 2009**, Hawaii, USA. E-Poster

4. DANKSAGUNGEN

Mein Dank gilt zunächst Dr. Tobias Saam und Professor Konstantin Nikolaou für das Angebot dieser Doktorarbeit und für meine Aufnahme in die Arbeitsgruppe „Plaqueimaging“ am Institut für Klinische Radiologie des Klinikums Großhadern. Das Engagement der Arbeitsgruppenleiter ist beispiellos und die erfolgreiche Publikation dieser Arbeit Resultat einer hervorragenden Zusammenarbeit. Ich möchte mich auch für die ausgesprochen freundliche Unterstützung meiner Mitdoktoranden Katja Bochmann und Andreas Schindler bedanken, da ohne deren Einsatz bei den MRT-Messungen das Projekt nicht möglich gewesen wäre. Auch gilt mein Dank Dr. Thomas Pfefferkorn, der das Projekt als Neurologe betreute und mit seiner klinischen Kompetenz eine unverzichtbare Hilfe war. Des Weiteren danke ich Prof. Chun Yuan für die herzliche Aufnahme in seine Arbeitsgruppe und lehrreiche Zeit während meines Forschungsaufenthalts am Vascular Imaging Laboratory in Seattle, USA. Zuletzt möchte ich mich bei Prof. Maximilian Reiser dafür bedanken, dass er die Teilnahme der Doktoranden an Kongressen förderte.

5. LEBENSLAUF

Maximilian Habs

geboren am 27.03.1984 in Heidelberg als Sohn von Prof. Dr. Dietrich Habs und Brigitte Habs.

Schulische Ausbildung

1990-1991	Internationale Gesamtschule Heidelberg
1991-1994	Strahlenberger Grundschule Schriesheim
1994-1995	Kurpfalz Gymnasium Schriesheim
1995-2003	Luitpold Gymnasium München
2003	Abitur

Studium

2005-2006	Studium der Chemie und Biochemie an der LMU München
2006	Beginn des Studiums der Humanmedizin an der LMU München
2008	Erster Abschnitt der Ärztlichen Prüfung
2009	United States Medical Licensing Examination Step 1
2010	Praktisches Jahr: <ol style="list-style-type: none">1. Chirurgie am Mount Sinai Hospital, New York und an der Chirurgischen Klinik Innenstadt der LMU München2. Innere Medizin am Nepean Hospital, Sydney und am Klinikum Innenstadt der LMU München3. Radiologie am Institut für Klinische Radiologie am Klinikum der LMU München
2012	Zweiter Abschnitt der Ärztlichen Prüfung

Promotion

- 2008-2011 Doktorarbeit in der Arbeitsgruppe „Plaque Imaging“ am Institut für Klinische Radiologie der LMU München. Leiter: Prof. Dr. Dr. h.c. Reiser
- 10/2009-01/2010 Forschungsaufenthalt am Vascular Imaging Laboratory, University of Washington, Seattle, USA. Leiter: Prof. Chun Yuan

Stipendien

- 10/2009-01/2010 DAAD-Stipendium für Forschungsarbeiten im Ausland (D/09/46101)
- 06/2011 Reisestipendium der DRG zum Deutschen Röntgenkongress

Sonstiges

- 2003-2004 Zivildienst am Klinikum Bogenhausen in München
- 2004-2005 Ausbildung zum Rettungssanitäter beim Bayerischen Roten Kreuz

Kontakt Daten

Maximilian Habs

Partnachstrasse 8

81373 München

Tel.: 0173-5645954

Email: Maximilian.Habs@gmail.com

München, den 10.08.2012